frontiers | Frontiers in Environmental Archaeology

TYPE Original Research
PUBLISHED 11 December 2023
DOI 10.3389/fearc.2023.1208985

OPEN ACCESS

EDITED BY
Grant Snitker,
New Mexico Consortium, United States

REVIEWED BY
João Carlos Ferreira Melo Júnior,
University of the Region of Joinville, Brazil
Michael Aiuvalasit,
University of Illinois at Urbana-Champaign, United States

*CORRESPONDENCE
S. Yoshi Maezumi
✉ maezumi@gea.mpg.de

RECEIVED 20 April 2023
ACCEPTED 10 November 2023
PUBLISHED 11 December 2023

CITATION
Maezumi SY, Power MJ, Smith RJ, McLauchlan KK, Brunelle AR, Carleton C, Kay AU, Roberts P and Mayle FE (2023) Fire-human-climate interactions in the Bolivian Amazon rainforest ecotone from the Last Glacial Maximum to late Holocene. *Front. Environ. Archaeol.* 2:1208985. doi: 10.3389/fearc.2023.1208985

Fire-human-climate interactions in the Bolivian Amazon rainforest ecotone from the Last Glacial Maximum to late Holocene

S. Yoshi Maezumi[1,2,3]*, Mitchell J. Power[2,3], Richard J. Smith[4], Kendra K. McLauchlan[5], Andrea R. Brunelle[3], Christopher Carleton[1], Andrea U. Kay[1], Patrick Roberts[1,6] and Francis E. Mayle[4]

[1]Department of Archaeology, Max Planck Institute of Geoanthropology, Jena, Germany, [2]Natural History Museum of Utah, University of Utah, Salt Lake City, UT, United States, [3]Department of Geography, University of Utah, Salt Lake City, UT, United States, [4]Department of Geography and Environmental Science, School of Archaeology, Geography and Environmental Science (SAGES), University of Reading, Reading, United Kingdom, [5]Department of Geography and Geospatial Sciences, Kansas State University, Manhattan, KS, United States, [6]isoTROPIC Research Group, Max Planck Institute of Geoanthropology, Jena, Germany

The Amazon Rainforest Ecotone (the ARF-*Ecotone*) of the southwestern Amazon Basin is a transitional landscape from tropical evergreen rainforests and seasonally flooded savannahs to savannah woodlands and semi-deciduous dry forests. While fire activity plays an integral role in ARF-*Ecotones*, recent interactions between human activity and increased temperatures and prolonged droughts driven by anthropogenic climate change threaten to accelerate habitat transformation through positive feedbacks, increasing future fire susceptibility, fuel loads, and fire intensity. The long-term factors driving fire in the ARF-*Ecotone* remain poorly understood because of the challenge of disentangling the effects of prolonged climatic variability since the Last Glacial Maximum (LGM; ~24,000 to 11,000 cal BP) and over 10,500 years of human occupation in the region. To investigate this issue, we implement an interdisciplinary framework incorporating multiple lake sediment cores, with varying basin characteristics with existing regional palaeoclimatological and archaeological data. These data indicate expansive C_4 grasslands coupled with low fire activity during the LGM, higher sensitivity of small basins to detecting local-scale fire activity, and increased spatial diversity of fire during the Holocene (~10,500 cal year BP to the limit of our records ~4,000 cal year BP), despite a similar regional climate. This may be attributed to increased human-driven fire. These data raise the intriguing possibility that the composition of modern flora at NKMNP developed as part of a co-evolutionary process between people and plants that started at the beginning of the ARE occupation.

KEYWORDS

palaeofire, indigenous burning, C4 vegetation, stable isotope analysis, macrocharcoal, last glacial maximum, biodiversity

1 Introduction

The Amazon rainforest is an expansive and vital biome that displays a diverse distribution of vegetation formations, including tropical rainforests, flooded grasslands, and dry savannahs, creating a mosaic of habitats essential for the region's unparalleled biodiversity. The Amazon Rainforest Ecotone (hereafter the ARF-*Ecotone*) of the southwestern Amazon Basin is a transitional landscape between the humid evergreen tropical forests (HETF), the seasonally flooded savannahs (SFS) of the Llanos de Moxos (Mayle et al., 2007), the upland (cerrado) savannahs, and the semi-deciduous tropical forests (SDTF) of Chiquitaniá. Fire plays an integral role in maintaining these vegetation transition zones, from fire-limited HETF to fire-prone SFS, SDTF and cerrado vegetation (Figure 1). Modern synergies between climate change (e.g., more frequent, severe droughts (Bowman et al., 2020) and human activity (e.g., increased deforestation for ranching, crop land expansion, and infrastructure development) threaten to accelerate forest die-back through positive-feedback loops by increasing future tree mortality, fire susceptibility, fuel loads, fuel connectivity and fire intensity (Doughty et al., 2015; Feldpausch et al., 2016; Le Page et al., 2017; Brando et al., 2020). These compounding factors have caused the ARF-*Ecotone* to become one of the most heavily exploited and most threatened regions of the Amazon (Cochrane, 2009; Le Page et al., 2017). This recent increase in fire activity is not just of regional significance, given that changes to the Amazon rainforest have been identified as one of the potential major future tipping points in the Earth's climate state (Lenton et al., 2019).

While fire is an ancient influence on the Earth system human agency has become increasingly important (Bowman et al., 2020). Today, humans are the primary cause of fire ignitions globally (Bowman et al., 2020; Pereira et al., 2022), and in fire-prone ecosystems including the SDTF and cerrado savannahs of the ARF-*Ecotone*, fires are more frequent when humans are in the landscape (Power et al., 2016; Le Page et al., 2017; Maezumi et al., 2018b; Brando et al., 2019). Indeed, as the keystone species of fire (Pyne, 2021), humans are the only species able to directly and deliberately manipulate fires through a variety of management practices (Levis et al., 2018; Bowman et al., 2020). Humans can shape fire directly, by manipulating the frequency, severity, and intensity of fires, and indirectly, by influencing the abundance and distribution of vegetation and through the introduction, cultivation, and domestication of plant species (Bowman et al., 2016, 2020; Levis et al., 2018; Hoffman et al., 2021; Furquim et al., 2023). For example, ethnographic studies demonstrate hunter-gatherers often influence vegetation structure, composition and diversity near human settlements (Posey and Balée, 1989; Politis, 1996; Denevan, 2006; ter Steege et al., 2013; Clement et al., 2015; Lins et al., 2015; Levis et al., 2018).

While the impact of humans on modern fire is substantial, the human use of fire to modify landscapes was practiced long before the colonization of the Americas (Boivin et al., 2016; Roberts et al., 2017). There is increasing evidence that in the Amazon, Indigenous traditional burning practices (hereafter Indigenous burning) influenced fire activity in mountain cloud forests (Loughlin et al., 2018), humid evergreen tropical forest (Bush et al., 2015, 2016; Carson et al., 2015; Maezumi et al., 2018a,b, 2022), semi-deciduous tropical forests (Bush et al., 2015; Carson et al., 2015), and cerrado savannahs (Carson et al., 2015; Brugger et al., 2016) as early as the mid-Holocene (~6500 cal year BP). The recent archaeological evidence documenting extensive human occupation in the Bolivian ARF-*Ecotone* region after ~10,500 cal year BP (Watling et al., 2018; Capriles et al., 2019; Lombardo et al., 2020), raises the possibility that human-fire linkages may have influenced fire activity in the region much earlier than previously proposed (Urrego et al., 2013; Carson et al., 2014; Bush et al., 2016; Maezumi et al., 2018b).

In light of the above, it is critical to obtain and compare multidisciplinary, direct proxy records of changes in past fire (hereafter palaeofire) regimes, vegetation change, human activity, and changes in key climate parameters in order to explore changing fire dynamics through time and their implications for future model projections. However, as a result of the complex fire-human-climate interactions and incomplete historical or long-term datasets (O'Connor et al., 2011; Bowman et al., 2020), the role of human-influences on palaeofires in the ARF-*Ecotone* remains largely unknown. While previous palaeoecological studies in the region have examined the relationship between basin characteristics (e.g., type/size) and fossil pollen archives (Smith et al., 2021), little is known about the relationship between basin characteristics and fossil charcoal records used to reconstruct past fire activity. We hypothesize that there is greater sensitivity of small lake basins to detect local-scale fire activity, thus smaller basins may be more sensitive to picking up Indigenous burning. To address this issue, we compare high-resolution (sub-centennial) Late Quaternary records from sites with varying basin characteristics. In addition to basin size, we explore potential drivers (e.g., climate, human) of the spatial and temporal variability of fire and vegetation change in the ARF-*Ecotone*. We implement a multi-proxy approach utilizing geochemistry, $\delta^{13}C$ and $\delta^{15}N$ stable isotopes, and macrocharcoal (>125 μm) analysis from a new ~24,000-year-old sediment core (Cuatro Vientos) that exceeds the earliest evidence of human activity in the region by > ~13,500 years. These data are compared with two existing palaeovegetation studies of Laguna Chaplin and Huanchaca Mesetta palm swamp in Mayle et al. (2000), Burbridge et al. (2004), and Maezumi et al. (2015, 2018b), along with regional palaeoclimate (Baker et al., 2001; Whitney et al., 2011) and regional archaeological data (Maezumi et al., 2018b; Capriles et al., 2019; Lombardo et al., 2020; Capriles, 2023; Peripato et al., 2023) (Supplementary Table S4).

2 Materials and methods

2.1 Study area

Noel Kempff Mercado National Park (NKMNP) is a 15,230 km^2 protected reserve located near the southern margin of the Amazon basin in the department of Santa Cruz, north-eastern Bolivia (14°22′9.336″, 60°51′14.3994″; Figure 1) (Killeen and Schulenberg, 1998). The park has been designated a UNESCO world heritage site due to its exceptionally high beta (habitat) diversity (Killeen et al., 2003; Heyer et al., 2018). The biodiversity of the park is attributed to the high

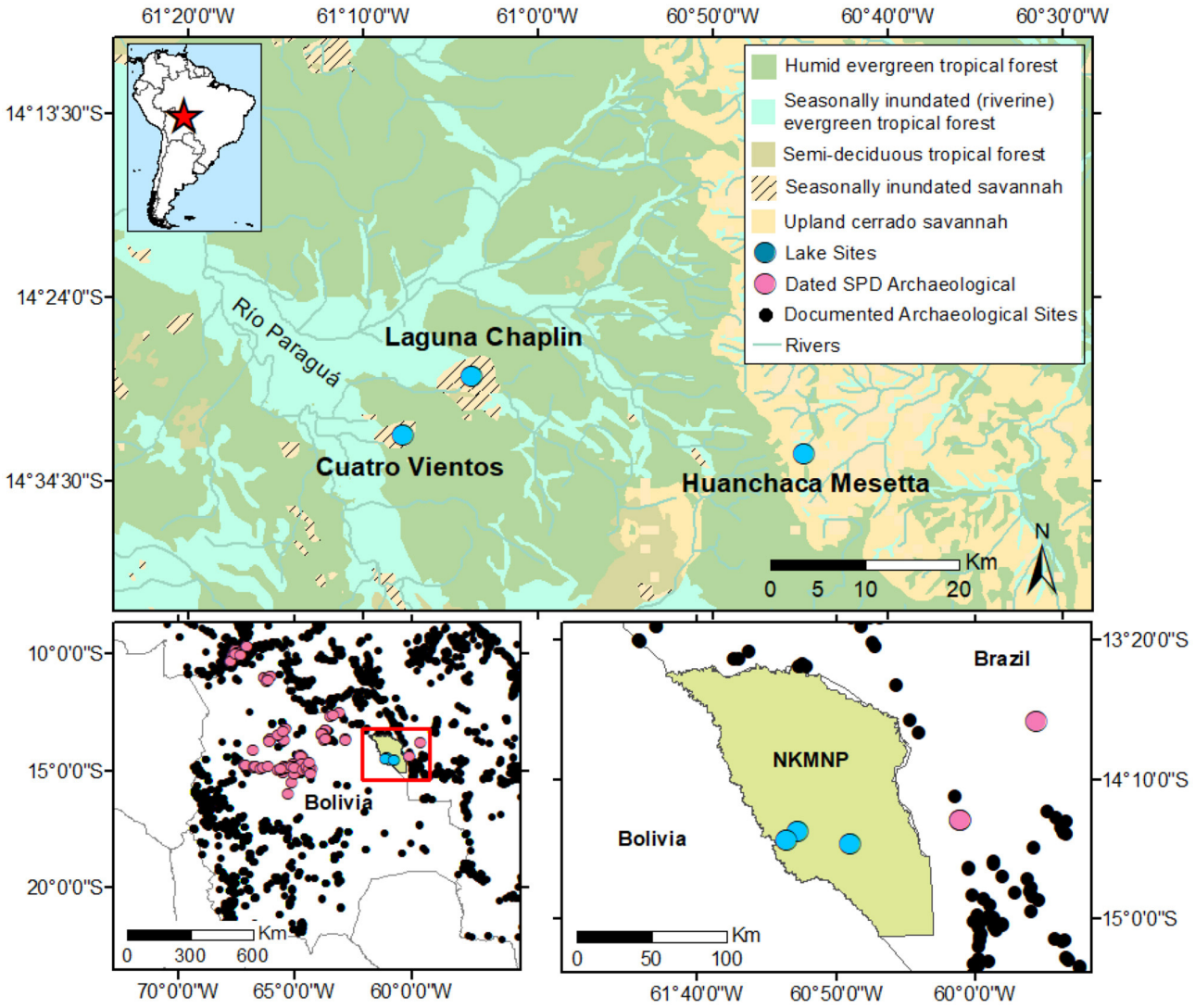

FIGURE 1
Regional Map of the study area in South America. Top vegetation map generated from Global Ecoregions, Major Habitat Types, Biogeographical Realms and The Nature Conservancy Terrestrial Assessment Units as of August 7, 2007 (Olson and Dinerstein, 2002) with insert map of South America with study region indicated by red star. Bottom left map Bolivia with regional AMS-dated archaeological sites included in the SPD analysis (pink dots), regional archaeology sites black dots from Bolivia (Capriles, 2023) and Brazil (Peripato et al., 2023), and lake study sites used in this study (blue dots). Bottom right map of Noel Kempff Mercado National Park (NKMNP) boundary (olive green) showing location of Cuatro Vientos, Laguna Chaplin, and Huanchaca Mesetta study sites (blue dots), dated archaeology (pink dots), and other archaeology sites documented in Brazil (Peripato et al., 2023).

levels of habitat heterogeneity which incorporates five distinct ecosystems: humid upland forest, inundated and riparian forest, semi-deciduous and deciduous forest, upland savannah and savannah wetland (Killeen and Schulenberg, 1998; Killeen et al., 2003; Burbridge et al., 2004). While the park is considered to be largely undisturbed by modern anthropogenic land use, ceramics have been recovered from a soil pit in an interfluve ~25 km northwest of our study sites and abundant ceramics mixed with charcoal (dated to ~400–500 cal year B.P.) were recovered from Amazonian Dark Earths throughout La Chonta (Guarayos province) ~150 km west of NKMNP (Burbridge et al., 2004). To date, no archaeological surveys or excavations have been conducted within NKMNP though there are, increasing numbers of archaeological sites identified in the surrounding region (Figures 1, 9, Supplementary Table S4).

2.2 Climate

The climate of NKMNP is characterized by a tropical seasonal climate with intermediate rainfall between increasingly moist regions to the north and the drier areas to the south (Killeen and Schulenberg, 1998). Mean annual precipitation at NKMNP is ca. 1,400–1,500 mm per year, with a mean annual temperature between 25 and 26°C (Centro de Previsão de Tempo e Estudos Climáticos, Instituto Nacional de Pesquisas da Amazônia [CPTEC/INPA], 2023). There is a 3–5 months dry season during the austral winter, when the mean monthly precipitation is <30 mm (CPTEC/INPA) Precipitation falls mainly during the austral summer, originating from a combination of deep-cell convective activity in the Amazon Basin from the South American summer monsoon (SASM) and the Intertropical Convergence Zone (ITCZ) (Vuille et al., 2012;

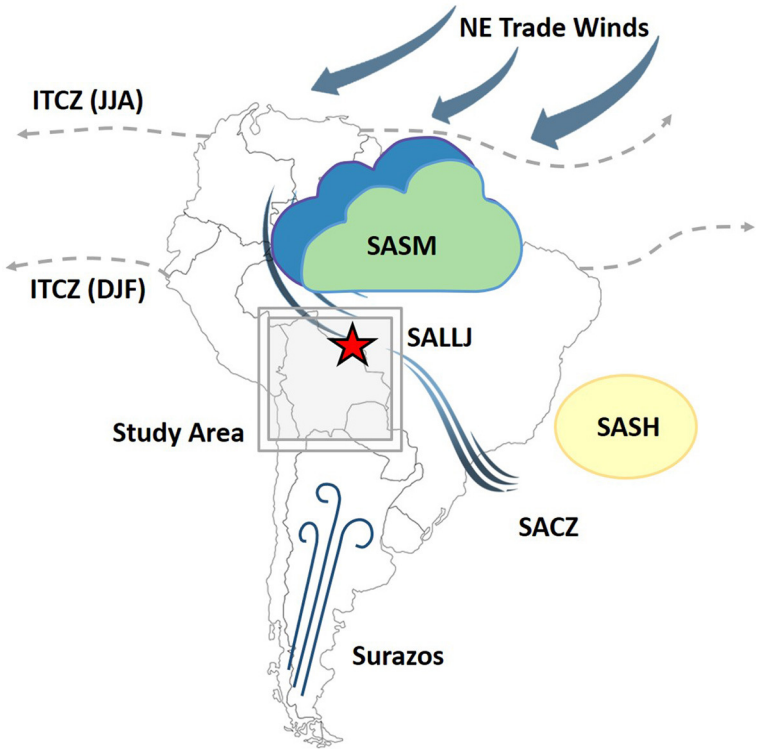

FIGURE 2
Schematic features of the tropical and subtropical South American climate including the Intertropical Convergence Zone (ITCZ) in June-July-August (JJA) and December-January-February (DJF), the South American summer monsoon (SASM), the South American low-level jet (SALLJ), the South Atlantic Subtropical High (SASH), the South Atlantic convergence zone (SACZ), and the cold, dry polar advections from Patagonia, locally known as *surazos*.

Novello et al., 2017; Orrison et al., 2022) (Figure 2). The SASM transports Atlantic moisture into the basin and corresponds to the southern extension of the ITCZ driven by seasonal variation in insolation (Bush and Silman, 2004; Vuille et al., 2012). When the ITCZ is located over the equator or further south, the northeast trade winds shift southward and intensify over South America. Diversion of the South American low-level jet (SALLJ) along the eastern foothills of the Andes delivers convective moisture from the Amazon basin to the La Plata Basin. The SALLJ converges with the western edge of the South Atlantic Subtropical High (SASH) and south-south westerly mid-latitude flow to form the South Atlantic convergence zone (SACZ), bringing precipitation to south-eastern Brazil during the austral summer (December to February). During the austral winter, cold, dry polar winds from Patagonia, locally known as *surazos*, can move northward, penetrating the NKMNP region causing temperatures to drop to 5–10°C for several days at a time (Latrubesse et al., 2012; Mayle and Whitney, 2012).

2.3 Geomorphology and regional vegetation

NKMNP is located on the western reach of the Precambrian Brazilian shield. The eastern half of the park is dominated by the Huanchaca Plateau, a table-mountain ~600–900 m above sea level (a.s.l) comprised of Precambrian sandstone and quartzite (Killeen, 1998). The plateau is dominated by upland cerrado savannah vegetation (Killeen and Schulenberg, 1998). To the west lies a lowland peneplain, where the Precambrian bedrock is overlaid by Tertiary and Quaternary alluvial sediments (Killeen, 1998) which is dominated by HETF vegetation. The Río Iténez and Río Paraguá black-water rivers form the northeastern and western boundaries of NKMNP, respectively. Today, these rivers are lined by riverine evergreen tropical forests with patches of seasonally-inundated savannah in areas where soil drainage is poor (Smith et al., 2021). The southern border of NKMNP defines the modern ARF-*Ecotone* between the southern Amazonian HETF and the Chiquitano semi-deciduous tropical dry forest (SDTF) of eastern lowland Bolivia (Killeen et al., 2003; Smith et al., 2021).

2.4 Site descriptions

In this study we compare high-resolution (sub-centennial) Late Quaternary charcoal records from three sites in NKMNP with varying basin characteristics (Figure 1). The first site, Cuatro Vientos (CV; 14°31′18.5″S, 61°7′11.3″W; ca. 184 m a.s.l.) is a small-sized (~5 km^2 area) palm swamp located in the western portion of NKMNP. CV is dominated by HETF to the east and the riparian forest of the Río Paraguá to the west (Smith et al., 2021). Growing within the CV basin itself is a floating mat of sedge/grass swamp vegetation, interspersed with small pools of

open water and scattered clumps of Arecaceae (palms) dominated by *Mauritiella* sp. A recent study of CV (Smith et al., 2021) demonstrates that palm swamps can yield Quaternary pollen archives recording terrestrial vegetation histories beyond the basin margin. To complement the previously published pollen data, here we conducted geochemical, stable carbon ($\delta^{13}C$) and nitrogen ($\delta^{15}N$) isotope, and macrocharcoal analysis from the same CV sediment core.

The second study site is Laguna Chaplin (LCh, 14°28′12″S, 61°2′60″W; elevation ~170 m a.s.l.), a large (~12 km^2), shallow (2–2.5 m in the dry season), flat-bottomed lake (within a ~20 km^2 basin) located ~6.5 km north-east of CV (Mayle et al., 2000; Burbridge et al., 2004). Today, LCh is surrounded by HETF, with a mix of seasonally-inundated riverine forest and *terra firme* (upland) HETF. Previous pollen and charcoal studies of LCh have documented evidence of climate-driven ecotonal dynamics that replaced flammable SFS with less flammable HETF vegetation, maize crop cultivation, and Indigenous fire use during the Holocene (Mayle et al., 2000; Burbridge et al., 2004; Maezumi et al., 2018b).

The third study site is Huanchaca Mesetta (HM, 14°32′10.66″S, 60°43′55.92″W; elevation: 800 m a.s.l.), a small palm swamp (0.02 km^2 area) located on the eastern portion of NKMNP atop the Huanchaca table mountain ~40 km east of CV (Figure 1). HM is comprised of a monospecific stand of *Mauritia flexuosa* palms. While previously published changes in vegetation composition and fuel loads have been documented in phytolith and charcoal data from within the HM palm swamp during the Holocene (Maezumi et al., 2015), the broader table mountain has likely been dominated by edaphically constrained cerrado savannah vegetation for millions of years as a result of the rocky substrate and lack of soil on the table mountain (Killeen and Schulenberg, 1998; Mayle and Whitney, 2012). To date, no archaeological or palaeoecological evidence of human occupation or fire use has been recorded on the table mountain (Maezumi et al., 2015). Based on limited archaeological research on the table mountain, we assume that the 14,500-year-old charcoal record from HM represents a natural, lightning-caused cerrado savannah fire regime (Maezumi et al., 2015). HM is thus used as a general estimate of natural lightning-caused ignitions in the NKMNP region, serving as a "control" site to explore the possible influence of human-caused ignitions at LCh and CV.

2.5 Sediment core

A sediment core from CV palm swamp was collected in August 1995 by FM using a Livingstone modified square-rod piston corer (Wright, 1967) ~300 m from the eastern edge of the palm swamp and described in detail in Smith et al. (2021). The top 20 cm of the core was comprised of a floating mat of sedges and grasses. The 0 cm mark for collecting the core was the surface of the floating mat of grass and sedge which was ~30 cm thick. The water-sediment interface was between 30 cm depth and 155 cm depth. Sediments were solid enough to recover between 155 cm and 309 cm depth. The CV sediment cores were photographed and lithological descriptions were based on Munsell soil color charts and the texture of the sediment core (Figure 3). Visual descriptions, including sediment type, structure, texture, and organic content were undertaken to assist interpretation of the palaeoenvironmental data and comparisons with LCh and HM.

2.6 Chronology

The chronological framework for CV is based on nine Accelerator Mass Spectrometry (AMS) radiocarbon (^{14}C) dates originally published by Smith et al. (2021) (Figure 3; Supplementary Table 1). Because of the lack of sufficient plant macrofossils, the majority of the dates were obtained from non-calcareous bulk sediment. However, two of the samples (Beta-467884 and Beta-467885) contained enough decayed plant remains following pre-treatment to be dated. All samples selected for dating were treated to remove carbonates, and the plant remains were treated to remove mobile humic acids. The radiocarbon ages were calibrated using the IntCal20 calibration curve (Reimer et al., 2020), and an age-depth chronology was constructed using the Bayesian age modeling software Bacon v2.3.4 (Blaauw and Christen, 2011). As per previous studies (Whitney et al., 2011; Smith et al., 2021), the IntCal20 calibration curve was selected over SHCal20 because of the hydrological connection of the study area to the northern hemisphere, via the SASM (McCormac et al., 2004; Hogg et al., 2013).

2.7 Magnetic susceptibility

Magnetic susceptibility (MS) was measured to identify mineralogical variation in the sediments (Nowaczyk, 2001). The MS of sediments reflects the relative concentration of ferromagnetic (high positive MS), paramagnetic (low positive MS), and diamagnetic (weak negative MS) minerals or materials. Shifts in the magnetic signature of the sediment can be diagnostic of a disturbance event (Gedye et al., 2000). Sediment cores were scanned horizontally, end to end, at 1 cm intervals using a Barrington ring sensor equipped with a 75 mm aperture. Data were calibrated by removing background noise at the beginning and end of each core.

2.8 Loss on ignition

The variability in the organic content of the sediments was used, in conjunction with magnetic susceptibility measurements, to identify periods of variability in sediment composition and organic content throughout the sediment record. Loss-on-ignition (LOI) analysis was carried out at 4 cm intervals through the CV core. After drying at 100°C for 24 h, each 1 cm^3 sample was combusted at 550°C for 2 h (LOI550). The relative loss of weight before and after combustion determines the percentage organic carbon content that was present in that sample (Dean Jr, 1974; Heiri et al., 2001).

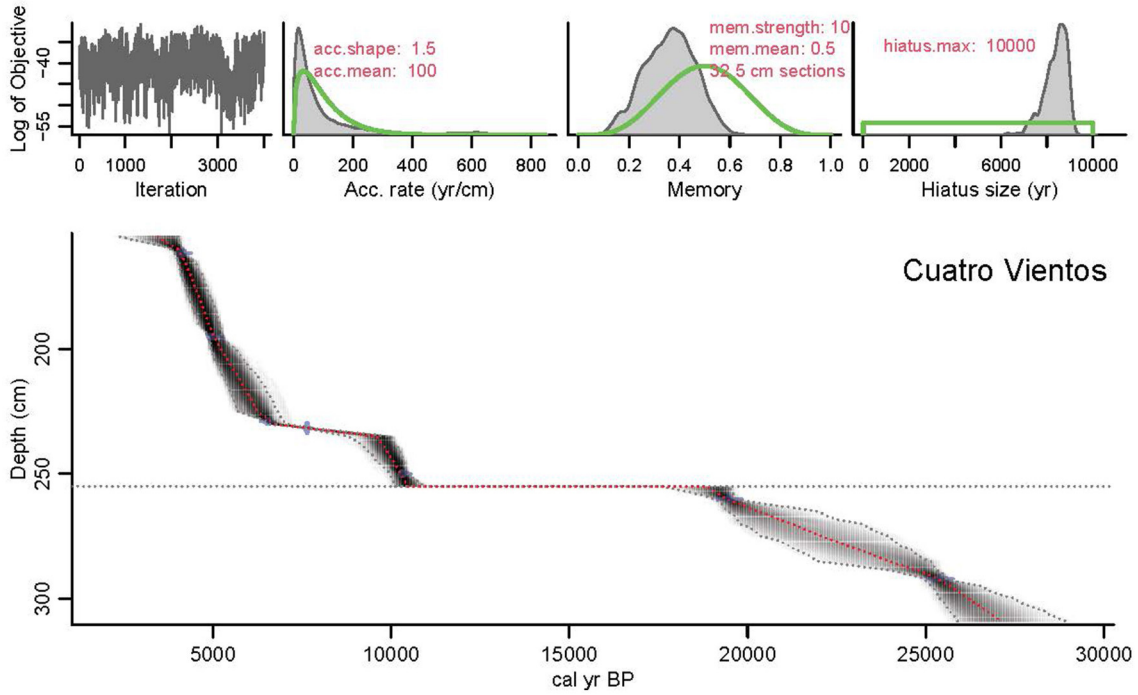

FIGURE 3
Cuatro Vientos age-model: the chronology for the sediments of Cuatro Vientos. **(Upper left panel)** Depicts the Markov Chain Monte Carlo (MCMC) iterations, priors (green curves) and posteriors (gray histograms) for accumulation rate **(top middle)** and memory **(top right)**. **(Lower panel)** Shows the calibrated ^{14}C dates and the age-depth model (darker grays indicate more likely calendar ages; gray stippled lines show 95% confidence intervals; red dashed curve shows single "best" model based on the weighted mean age for each depth. The Chronology is derived from Bacon using the IntCal20 calibration curve.

2.9 X-ray fluorescence

X-ray fluorescence (XRF) analysis of the sediment core was carried out using the ITRAX core scanner at Aberystwyth University at a step size of 2,000 or 5,000 μm. An intense micro-X-ray beam focused through a flat capillary waveguide was used to irradiate samples to enable both X-radiography and X-ray fluorescence (XRF) analysis. Data were acquired incrementally by advancing a split core, via a programmable stepped motor drive, through the flat, rectangular-section X-ray beam (Croudace et al., 2006). Results were normalized using *z*-scores for comparability (Figure 4).

2.10 Stable isotope analysis

Stable carbon (δ^{13}C) isotope analysis was performed as a proxy for changes in vegetation structure and composition. The carbon in soil organic matter (SOM) is mainly derived from plants, resulting in a δ^{13}C value that closely reflects that of the standing plant biomass (Ambrose and Sikes, 1991; Bond et al., 1994) and is primarily determined by the photosynthetic pathway of vegetation (Ehleringer et al., 1991; Ehleringer and Cerling, 2002; Sage, 2004). Previous research on δ^{13}C values from NKMNP and the surrounding region (Pessenda et al., 1998; Killeen et al., 2003; Mayle et al., 2007; Maezumi et al., 2015; Lombardo et al., 2019) have been used to determine the relative proportions of C_4 savannah grasses vs. C_3 woody and herbaceous vegetation based on differences in the discrimination of the C_4 and C_3 photosynthetic pathways against the heavier ^{13}C isotope during CO_2 fixation (Smith and Epstein, 1971). Open vegetation characterized by the predominance of C_4 grasses has a typical δ^{13}C signature between −16.0‰ and −10.0‰, whereas dense vegetation characterized by trees is usually dominated by the C_3 photosynthetic pathway with a δ^{13}C signature between −26.0‰ and −20.0‰ (Cerling, 1984), although the exact values of these distinctions have been shown to vary for the Amazon Basin (Tejada et al., 2020).

The interpretation of δ^{13}C measurements of bulk SOM from lake sediments can be complex, however. Firstly, bulk SOM δ^{13}C can be offset from the plant material from which it derives by +1–3‰ as a product of microbial action (Ehleringer et al., 2000). Though this offset cannot mask the non-overlapping differences between C_3 and C_4 taxa (Roberts et al., 2013), the relative changes in δ^{13}C values throughout a sequence are often more meaningful than absolute comparisons. Secondly, the terrestrial C_3 and C_4 distinction are potentially complicated by the presence of CAM plants, which can have δ^{13}C values overlapping with, or between, both of these photosynthetic pathways (O'Leary, 1981). Thirdly, variation in environmental conditions (e.g., aridity, temperature) has been shown to influence the δ^{13}C values of C_3 plants in particular (Ehleringer and Björkman, 1977; Sage and Kubien, 2007; Kohn, 2010). Finally, the bulk organic matter of lake sediments is a product not only of terrestrial vegetation

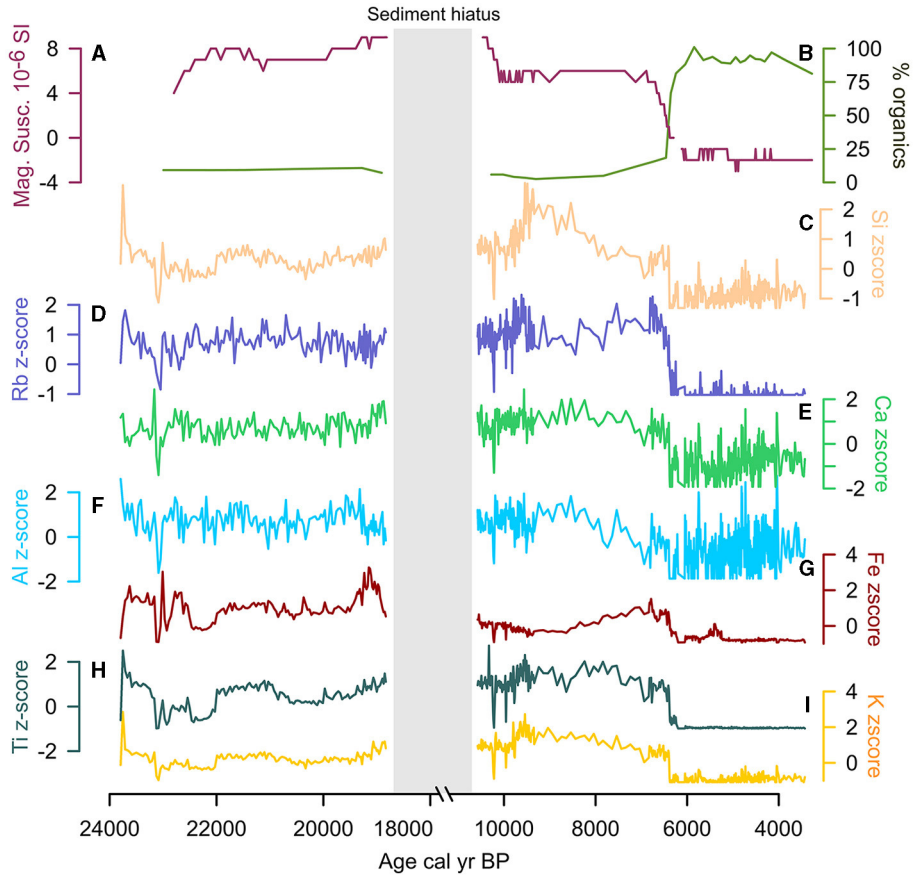

FIGURE 4
Cuatro Vientos XRF geochemical data from the Last Glacial Period to late Holocene: **(A)** Magnetic susceptibility, **(B)** Loss On Ignition (LOI), **(C)** Si *z*-score, **(D)** Rb *z*-score, **(E)** Ca *z*-score, **(F)** Al *z*-score, **(G)**, Fe *z*-score, **(H)** Ti *z*-score, **(I)** K *z*-score. *Y*-axis broken from 18,000 to 11,000 cal year BP during sediment hiatus.

in the catchment but also aquatic plants (Cloern et al., 2002) which can also follow C_3, C_4 or CAM pathways (Keeley and Sandquist, 1992). Additionally, carbon limitation tends to reduce carbon isotope discrimination resulting in higher $\delta^{13}C$ values in algae and submerged macrophytes (Sharkey et al., 1985; Keeley and Sandquist, 1992; Street-Perrott et al., 2004), making the teasing apart of terrestrial and lacustrine responses to climate and human activity complex. Consequently, comparisons with other, independent, records of vegetation and sedimentological conditions are essential.

Stable nitrogen ($\delta^{15}N$) isotope analysis provides an index of changing dynamics in the N cycle, particularly denitrification, as well as an indicator of the N_2-fixation processes. Plants, such as aquatic macrophytes (e.g., *Sagittaria*), can increase available N through N_2-fixation (Arima and Yoshida, 1982). Sediment $\delta^{15}N$ integrates a variety of nutrient cycling processes including the loss of inorganic N to the atmosphere through denitrification which results in the subsequent increases in $\delta^{15}N$ (Robinson, 1991; McLauchlan et al., 2013). Denitrification requires anaerobic conditions coupled with abundant available carbon and nitrate (Seitzinger et al., 2006). Thus, wet, anoxic sediments tend to have higher values of $\delta^{15}N$. Environmental conditions that alternate between wet (anaerobic) to dry (aerobic) conditions also lead to an increase in $\delta^{15}N$ values (Codron et al., 2005). During dry periods, denitrification is stopped because of an increase in available oxygen in sediments, and thus $\delta^{15}N$ values decrease. If dry soils become hydrated, there is a preferential loss of ^{14}N, increasing $\delta^{15}N$ values (Jordan et al., 1982; Codron et al., 2005). $\delta^{15}N$ values have also been associated with forest cover in the Amazon (Ometto et al., 2006) and in the anthropogenic enrichment of soils in Southern Africa (Aranibar et al., 2008).

Subsampling for stable isotope analysis was performed at 1.5-cm-resolution throughout the length of the sediment core (Figure 5). One cm^3 of bulk sediment was dried, powdered, and treated with 0.5 molar hydrochloric acid to remove carbonates. One to 25 mg of the dried carbonate-free sediment was weighed into tin capsules depending on organic matter content. Following reaction with 100% phosphoric acid, gases evolved from the samples were analyzed for stable carbon and nitrogen isotopic composition using a Finnigan Delta dual inlet elemental analyzer at the SIRFER Lab at the University of Utah. $^{13}C/^{12}C$ and $^{15}N/^{14}N$ ratios were presented in delta (δ) notation, in per mil ($^0/_{00}$) relative to the international scale standard used for

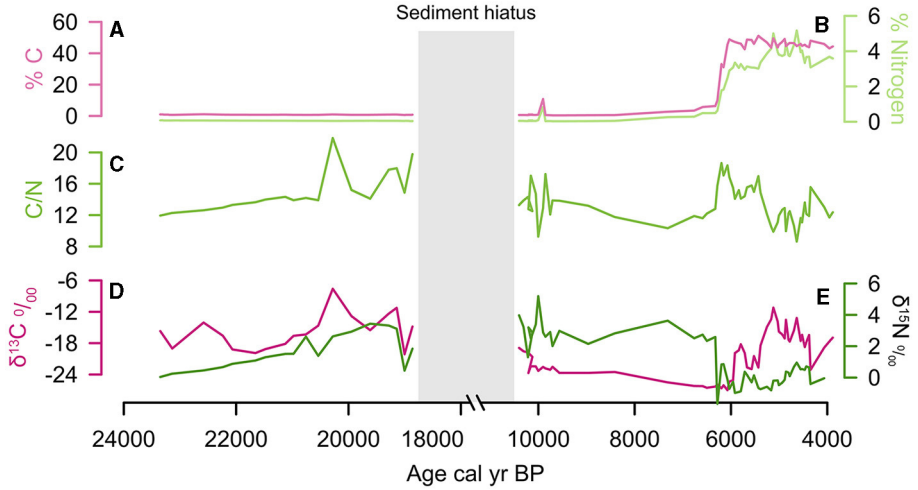

FIGURE 5
Stable carbon and nitrogen isotope data from Cuatro Vientos: **(A)** % Carbon, **(B)** % Nitrogen, **(C)** C/N ratio, **(D)** $\delta^{13}C$, **(E)** $\delta^{15}N$. *X*-axis broken from 18,000 to 11,000 cal year BP during sediment hiatus.

carbon, Vienna Pee Dee Belemnite (VPDB; USGS40 = $-26.24^{0}/_{00}$; USGS41 = $+37.76^{0}/_{00}$) and the standard for nitrogen, atmospheric N_{2AIR}(air) (USGS40 = $-4.5^{0}/_{00}$ and USGS40 = $-4.5^{0}/_{00}$) (Codron et al., 2005). $\delta^{13}C$ and $\delta^{15}N$ values were compared against International Standards [PLRM-1 ($\delta^{13}C_{VPDB}$ = +23.96‰; $\delta^{15}N_{AIR}$ = +49.63‰); PLRM-2 ($\delta^{13}C_{VPDB}$ = +28.18‰; $\delta^{15}N_{AIR}$ = −4.56‰); and SLRM MT soil ($\delta^{13}C_{VPDB}$ = +7.5‰; $\delta^{15}N_{AIR}$ = +16.96‰)]. Replicate analysis of SLRM standards suggests that machine measurement error is c. ± 0.2‰ for $\delta^{13}C_{VPDB}$ and ± 0.2‰ for $\delta^{15}N_{AIR}$. Overall measurement precision was studied through the measurement of repeat extracts from the SLRM standard.

2.11 Macrocharcoal

Sediment samples were analyzed for macrocharcoal pieces (>125 μm in minimum diameter) using a modified macroscopic sieving method (Whitlock and Larsen, 2001; Leys et al., 2015) to reconstruct the history of local and extra-local fires. Macrocharcoal was analyzed using 1 cm^3 volume of sediment in contiguous 0.5 cm intervals for the length of the sediment core. Samples were treated with 10% potassium hydroxide in a hot water bath for 15 min. The residue was sieved through a 125 μm sieve. Macroscopic macrocharcoal was counted in a gridded petri dish at 40× on a dissecting microscope. Macrocharcoal counts were converted to macrocharcoal concentrations (number of macrocharcoal particles cm^{-3}) and macrocharcoal influx rates by dividing by the deposition time (year cm^{-1}). CHAR statistical software was used to decompose charcoal data to identify distinct charcoal peaks using standard methodology (Higuera et al., 2007, 2009, 2010). Charcoal peaks are interpreted as a fire episode (a period of increased burning). The time difference between peaks is reflected in the fire return interval (fire frequency) for every 1,000 years.

2.12 Existing pollen data

The CV core was previously analyzed for pollen by Smith et al. (2021). Here, the Species Richness Index (SRI) was calculated from the existing pollen data which has previously been used to estimate floristic richness and biodiversity (Heck et al., 1975). Species richness was calculated from the total terrestrial fossil pollen data from CV (Smith et al., 2021) and LCh (Burbridge et al., 2004) using rarefaction analysis (Hurlbert, 1971; Heck et al., 1975) in the Vegan Community Ecology Package in R (Oksanen et al., 2017; R Core Development Team, 2020). Rarefaction enables the estimation of pollen richness using standardized pollen counts (Birks and Line, 1992). Standardization is important as palynological richness depends in part on the pollen sum because, as the sum increases, more taxa can potentially be detected. The units of rarefaction analysis represent the estimated number of pollen taxa reduced to a certain pollen sum, usually the lowest sum of the group of samples being compared.

2.13 Laguna Chaplin and Huanchaca Mesetta sediment cores

For complete palaeoecological analyses of LCh and HM see Mayle et al. (2000), Burbridge et al. (2004), and Maezumi et al. (2015, 2018b). Details on the recalibrated age-models follow. LCh and HM were cored in 1998 and 1995 by FM, with the results of the palaeoecological analyses presented in subsequent publications (Mayle et al., 2000; Burbridge et al., 2004; Maezumi et al., 2015, 2018b). Here, we replot the LCh and HM macrocharcoal and stable carbon isotope data with updated Bayesian age-depth models (Blaauw et al., 2018). The chronological framework for LCh presented here is based on 14 Accelerator Mass Spectrometry (AMS) radiocarbon (^{14}C) dates (Supplementary Table 2, Supplementary Figure 1) and six AMS

radiocarbon dates for HM (Supplementary Table 3, Supplementary Figure 2). Updated age models implement the Bacon Bayesian age modeling software package using the IntCal20 calibration curve (Reimer et al., 2020). CV, LCh, and HM are plotted from 24,000 to 3,500 to allow direct comparison with the 24,000-year CV macrocharcoal and isotope record.

2.14 Regional archaeological activity

The absence of archaeological sites in NKMNP, and the broader region of eastern Santa Cruz, the largest department in Bolivia, is attributed to the lack of systematic archaeological research in the region (Capriles, 2023). To the eastern edge of the park, across the Brazilian boarder, there are over 50 archaeological sites documented <50 km from the KNMNP (Figure 1). Additionally, recent maximum entropy models estimate 85% likelihood of pre-Columbian earthworks in the surrounding area (Peripato et al., 2023). Thus, in the absence of archaeological excavations and surveys within NKMNP, we relied on existing, regional archaeological data (Figure 1). We infer that these data are representative of NKMNP as these dated archaeological sites come from analogous settings across the *ARC-Ecotone* including sites that are coupled with palaeoecological studies documenting crop cultivation and agroforestry (including maize cultivation, similar to LCh) and Indigenous burning (Carson, 2014; Brugger et al., 2016; Maezumi et al., 2022). Additionally, the archaeological ceramics present within an interfluve ~25 km northwest of our study sites are similar to ceramics documented outside of the park (Riester, 1981; Carson et al., 2014; Barreto et al., 2016; Maezumi et al., 2022).

Identifying change in regional human activity levels and population size over time is frequently done with a "dates-as-data" approach (Rick, 1987). Under this paradigm, the abundance of dated archaeological deposits is thought to correlate over time with regional human activity in the sense that more dated deposits (more dates) in a given time and place indicates more human activity. This logic holds because a change in activity levels and/or an increase in population corresponds (though imperfectly correlated), to a change in the abundance of datable deposits entering the archaeological record at a given place and time. Following this logic, we compiled a radiocarbon date database (Supplementary Table S1) comprising archaeological deposits across the Bolivian ARF-ecotone into the Llanos de Moxos savannah ranging from 19,500 BP to 3,500 BP. We compared the abundance of those dates to our palaeoecological proxies for CV, LCh, and HM. The aim was to evaluate if regional human activity corresponded to changes in the palaeoecological record (i.e., fire activity).

To accomplish this, we used two visualizations to summarize the information contained in the radiocarbon database. The first visualization is Summed Probability Density (SPDs). SPDs have frequently been used as an indirect proxy for identifying change over time in human activity and demographic patterns (Shennan et al., 2013; Bevan et al., 2017; Ramsey, 2017). They are produced by calibrating each date in a given sample and then summing the probability distributions to produce a single density curve. That curve represents the temporal distribution of events in the relevant database along with their combined chronological uncertainty (Shennan et al., 2013; Timpson et al., 2014; Downey et al., 2016; Goldberg et al., 2016; Zahid et al., 2016). While popular, SPDs have significant limitations. Crucially, they conflate temporal event density or count with dating uncertainties and should largely serve only as a visual aid with some significant caveats regarding biases, calibration artifacts, and their point-wise interpretation (Carleton and Groucutt, 2021; Price et al., 2021; Crema, 2022). Nevertheless, they have become a staple of regional archaeological syntheses and can be deployed to help visualize the overall distribution of anthropogenic deposits and their relevant dating uncertainties in relation to other proxies.

The second visualization used here is called a Radiocarbon-dated Event Count Ensemble (RECE). A RECE provides visual information along three dimensions: one is time, another is count, and the other is probability (Carleton, 2021; Carleton and Groucutt, 2021). The ensemble refers to a collection of randomly sampled, probable event count time series that can be produced given a sample of radiocarbon dates. The dates are first calibrated, and then the calibrated dates are sampled at random in proportion to their densities producing a probable set of event dates. Each time the set of calibrated radiocarbon densities is sampled, the sampled event dates are then binned at a given resolution into a pre-determined temporal grid in order to count the number of events (dates, and by extension dated deposits) that fall into each bin. This produces an event count time series at the given resolution. The process is then repeated (i.e., 10,000 times) to produce the ensemble. A 2d grid histogram, is created where one axis represents time corresponding to the selected bin resolution and the other axis represents event count. The ensemble is then coded on the 2d grid based on the probable count sequence for each bin. These relative frequencies are then visualized with a heat-map spectrum so that the final image (i.e., the plotted RECE) provides a visual of the most likely count sequences along with uncertainty about both count and time in a single image. In this way, RECEs can help to separate event abundance from chronological uncertainty, suffer less from calibration artifacts than SPDs, have a clearer interpretation for comparison with other proxies, and indicate both overall sample size (maximum counts in one dimension) and total uncertainties in two dimensions.

To produce these visualizations, a total of 418 AMS dates were compiled from 98 archaeological sites from the Bolivian lowlands (ca. 69°-58°W, 9°-16°S; Supplementary Table S3). A binning procedure was applied to account for sites that have multiple dates within a phase (Shennan et al., 2013; Timpson et al., 2014; Goldberg et al., 2016). Dates within sites were ordered and those occurring within 100 years of each other were grouped into bins and merged. Each bin had a maximum width of 200 years. SPDs were then built in the package "rCarbon" (Crema and Bevan, 2021) and a RECE plot was produced using the package "chronup" (Carleton, 2021) using the IntCal20 calibration curve (Reimer, 2020; Reimer et al., 2020). In response to recent critiques of the SPD method such as minimum sample size ($n = 500$) (Williams, 2012) and the conflation of chronological uncertainty (Carleton and Groucutt, 2021), we refrain from interpretations about past population levels, and rather use the SPD curve and RECE plots as indicators of human presence in the region at a coarse temporal resolution with no reference to rates of change or palaeodemographics.

3 Results

The CV Bacon age-depth model was derived from seven of the nine AMS-radiocarbon dates and has previously been published (Smith et al., 2021), although here we update the chronology using the IntCal20 calibration curve (Reimer et al., 2020). The dates at 240 cm and 276 cm were rejected based on the outlier identification in Bacon. Ages for the top 160–155 cm and bottom 292 to 309 cm of the core were based on interpolation and extrapolation. The lithology of CV, as described in Smith et al. (2021), was divided into three main stratigraphic sections (Figure 3): (1) the Last Glacial Period (309–255 cm; 24,000–11,000 cal year BP), (2) the early to middle Holocene (255–230 cm; 11,000–7,000 cal BP), and (3) the middle to late Holocene (230–155 cm; 7,000–3,700 cal year BP). These three stratigraphic sections provide the chronological framework for discussing the new MS, LOI, XRF, stable carbon and nitrogen isotope, and macrocharcoal results from CV.

3.1 Last glacial period (24,000–11,000 cal year BP; sediment hiatus 18,000–11,000 cal year BP)

Magnetic susceptibility (MS) values from CV ranged between 4 and 8 and <10% organic material was present, as indicated by the LOI values. The XRF data indicated high frequency, low amplitude variability in Si, Rb, Ca, AL, Fe, Ti, and K (Figure 4). These data suggest a higher energy, nutrient-poor environment that may have been associated with substantial riverine influence. The pollen during this period suggests abundant Poaceae (grass 40%−60%) and Cyperaceae (sedge, 5%−10%) presence, along with cold adapted taxa including Podocarpaceae (*Podocarpus*), Betulaceae (*Alnus*), and Aquifoliaceae (*Ilex*). The savannah indicator *Curatella americana* (Dilleniaceae) was present *(<1%)*. Only a few grains of the aquatic/semi-aquatic taxa from Alismataceae (*Sagittaria* sp.) and Isoetaceae (*Isoetes* sp.) were recovered (Smith et al., 2021). Pollen data are summarized in Figure 6.

Total %N remains low (<0.1%) and $\delta^{15}N$ ranges between −0.6 and 3.4‰. Total %C was low (<1%) and the $\delta^{13}C$ values range between −16.0 to −8.0‰, indicating the highest contribution of C_4 vegetation in the CV record during this period (Figure 5). The $\delta^{13}C$ values at LCh (−18.0) and HM (−18.0 to −16.0‰) also indicate a contribution of C_4 vegetation at this time. The C/N values at CV fluctuate between 14 to 22 (Figures 6, 7), suggesting a mixed contribution of aquatic (∼10) and terrestrial (∼20) organic sources The existing palynological data from CV and LCh (Figure 8) indicate open, seasonally flooded savannah (Burbridge et al., 2004; Smith et al., 2021). The lack of phytolith preservation at HM prior to 15,000 cal year BP limits vegetation reconstruction on the table mountain (Maezumi et al., 2015). The absence of phytolith preservation at HM was attributed to the limited vegetation growing within the small palm swamp basin. Nevertheless, the $\delta^{13}C$ values (−19 to −15‰, Figures 7, 8) suggest C_4 grasses were growing on the table mountain. The sediment hiatus between ∼18,000 and 11,000 cal year BP at CV is synchronous with low sedimentation rates (∼0.02 mm $year^{-1}$) at LCh (Burbridge et al., 2004) and a sediment hiatus at HM from ∼18,000 to 16,000 cal year BP (Maezumi et al., 2015). Despite the presence of C_4 fire-adapted vegetation, such as grasses, macrocharcoal values were low at all three sites during this period. Human activity in the region was minimal between 19,500 and 11,000 cal year BP based on the regional radiocarbon dated archaeological sites (Figure 9).

3.2 Early to middle Holocene (11,000–7,000 cal year BP)

The end of the sediment hiatus at CV ∼11,000 cal year BP (Figure 3) was associated with decreased MS values from ca. 8 to 4 ∼10,000 cal year BP (Figure 4), suggesting a shift to a lower energy depositional environment. LOI values remained <10% indicating a continuation of organic-poor sediments. The XRF data, particularly Si, exhibits greater amplitude variability after 10,000 cal year BP, reaching record high values (∼3) between 10,000 and 8,000 cal year BP that correspond with a sand layer (Figure 4). These lithological changes were likely associated with changing fluvial dynamics and greater riverine influence that increased Si-rich sand deposition at CV. The sand layer corresponds to poor pollen preservation at CV between 8,750 and 7,000 cal year BP (Smith et al., 2021; Figure 8).

Total % N remained low (<0.1) and $\delta^{15}N$ values increased slightly from the previous period (1.0 and 5.0‰). Total % C was low (<1%) and the $\delta^{13}C$ values indicate a progressive replacement of C_4 vegetation with C_3 vegetation at all three sites toward the late glacial-Holocene transition (Figures 6, 7). Coupled with an increase in C/N values (∼16‰), these data indicate increased terrestrial organic matter input at CV (Figures 5, 6). Fire activity NKMNP increases at HM ∼ 12,000 to 9,000 cal year BP and at CV ∼10,500 to 9,600 cal year BP, indicated by charcoal influx and fire frequency values (Figures 6, 9). Macrocharcoal values remain low at LCh (<1) throughout this period. Fire activity was low between ∼9,000 and 6,500 cal year BP at CV and LCh, (<2) coupled with a sediment hiatus at HM from ∼9,000 to 8,300 cal BP prior to the onset of the mid-Holocene Dry Period (MHDP; 6,000–4,000 cal year BP). The SPD and RECE values indicate increased human activity at this time (Figure 9, Supplementary Figure S3).

3.3 Middle Holocene (7,000–3,700 cal year BP)

Around 6,500 cal year BP there were abrupt declines in MS (6 to −2) and an increase in organic content (>90%) at CV (Figure 4). This was synchronous with declines in Si, Rb, Fe, Ti and K values. Ca and Al exhibit higher frequency and greater amplitude variability after ∼6,000 cal year BP. Pollen data show the presence of a dry forest-savannah mosaic during this time period (Smith et al., 2021). The aquatic/semi-aquatic taxa *Sagittaria* and *Isoetes* increase, with *Sagittaria* becoming a large proportion of the total pollen sum (∼20%) between ca. 6,000–5,500 cal year BP (Figure 8). The increase in the aquatic C_4 plant *Sagittaria* corresponds to a shift in $\delta^{13}C$ values at CV (from −24.0 to −12.0). These data correspond with low C/N values (<12; Figures 5, 7), indicating a greater contribution of aquatic vs. terrestrial carbon input. The increase in sediment organic matter at CV during this period

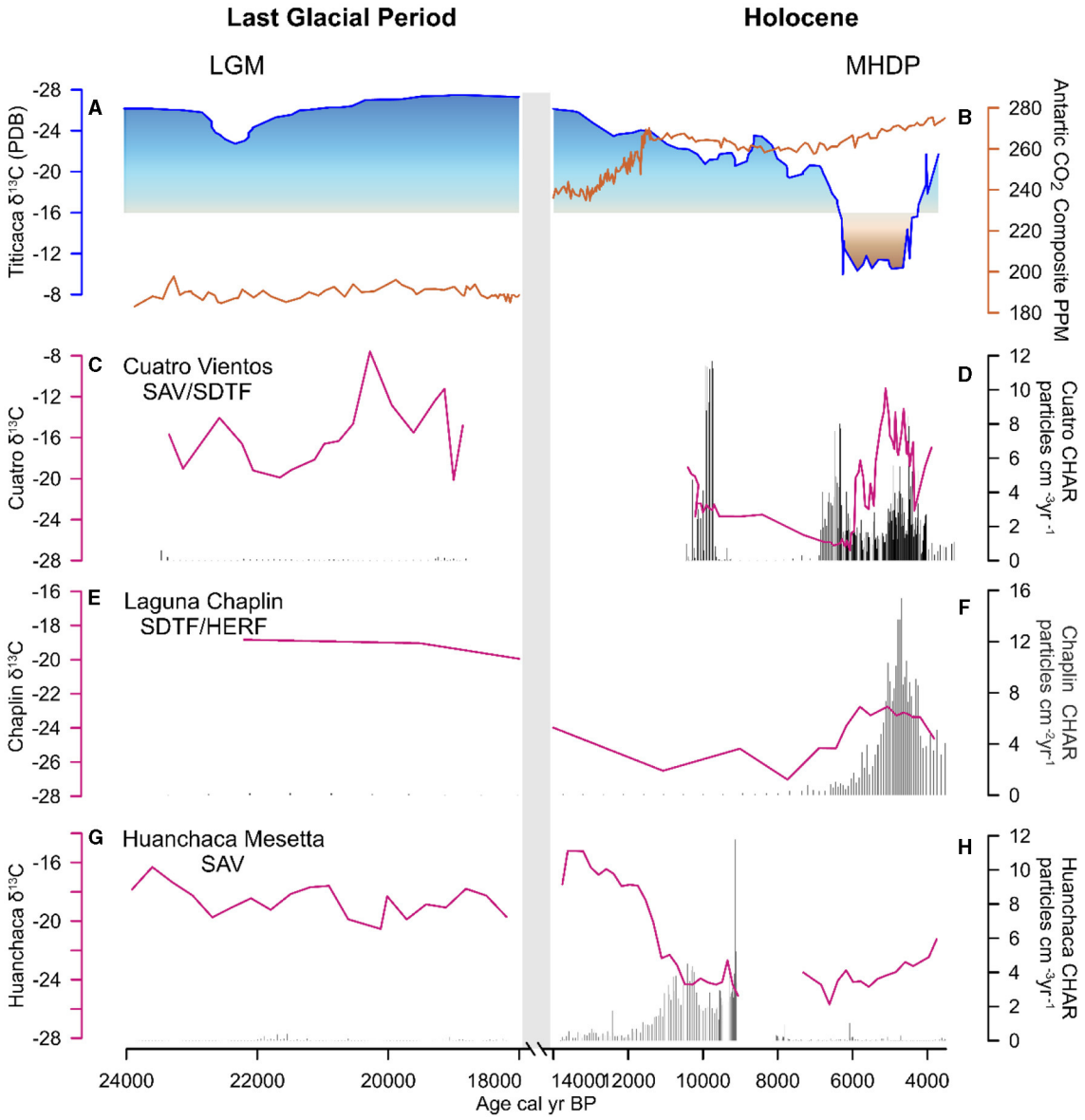

FIGURE 6
Regional climate, charcoal, and stable carbon isotope measurements: **(A)** Lake Titicaca lake levels (Baker et al., 2001), **(B)** Antarctic CO_2 concentrations, **(C)** $\delta^{13}C$ Cuatro Vientos, **(D)** Cuatro Vientos charcoal accumulation, **(E)** $\delta^{13}C$ Laguna Chaplin, **(F)** charcoal accumulation Laguna Chaplin, **(G)** $\delta^{13}C$ Huanchaca Mesetta, **(H)** charcoal accumulation Huanchaca Mesetta. *X*-axis broken from 18,000 to 14,000 cal year BP during sediment hiatus. LGM, Last Glacial Maximum; MHDP, Mid-Holocene Dry Period.

suggests a shift toward more eutrophic conditions indicating lower water levels (Smith et al., 2021).

Between 6,000 and 4,000 cal year BP the $\delta^{13}C$ values at LCh also indicate an increase in C_4 vegetation (Figure 6) that was not associated with a significant increase in grass pollen (Figure 8), that did correspond to a 10% increase in the aquatic CAM plant, *Isoetes* which has higher $\delta^{13}C$ values (−20 to −10‰) compared to woody C_3 vegetation (<-24‰).

The MHDP was associated with increased variability of fire between CV, LCh, and HM. There was an increase in fire activity at CV ~6,500–6,000 cal year BP indicated by higher charcoal influx and fire frequency values that were not documented at LCh despite similar SDTF vegetation (Figures 8, 9) and close proximity (~5 km) of the lakes. At both CV and LCh there was a negative correlation between pollen species richness and increased macrocharcoal (Figure 8). This corresponds with an increase in human activity ca. 6,500 and 5,000 cal year BP indicated by a rise in SPD and RECE values (Figure 9). Fire activity at HM was low to absent during this period, despite abundant available fuel indicated by the presence of ca. 80% woody vegetation documented in the phytolith data (Figure 8). Fire increased between 5,000 to 4,000 cal year BP at CV and LCh, followed by decreased fire at both sites after ~4,000 cal year BP.The CV record terminates at 3,750 cal year BP, prior to the establishment of modern palm swamp vegetation.

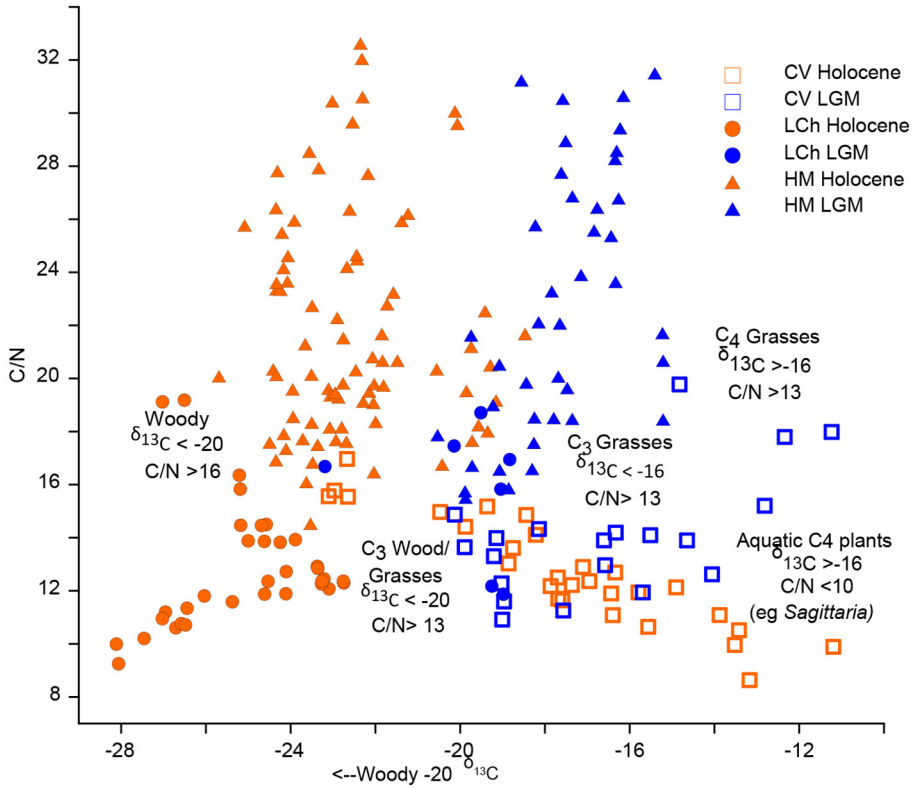

FIGURE 7
Biplot of C/N ratio to stable carbon ($\delta^{13}C$) isotope measurements for Cuatro Vientos (CV), Laguna Chaplin (LCh), and Huanchaca Mesetta (HM) for the Holocene and Last Glacial Maximum (LGM). CV Holocene: open orange square, CV LGM: open blue square, LCh Holocene: orange circle, LCh Holocene: blue circle, LCh LGM: blue circle, HM Holocene: orange triangle, HM LGM: blue triangle.

4 Discussion

4.1 Climate and ARF-ecotone vegetation dynamics during the last glacial period (24,000–11,000 cal year BP)

During the Last Glacial Maximum (LGM; ~21,000 cal year BP) atmospheric CO_2 levels were ~76 ppm lower (Monnin et al., 2001), temperatures were ~5°C cooler than pre-industrial values (Seltzer et al., 2002; Whitney et al., 2011; Metcalfe et al., 2014), and decreased precipitation, in response to lower evaporative moisture, resulted in drier than present conditions across tropical lowland South America (Burbridge et al., 2004; Whitney et al., 2011; Woillez et al., 2011; Novello et al., 2019; Orrison et al., 2022). C/N values (>12) and $\delta^{13}C$ (−16 to −12‰; Figures 7, 8), combined with the low abundance of C_4 aquatic plants documented in the pollen records, suggest that C_4 terrestrial vegetation dominated the NKMNP landscape between the LGM and onset of the Holocene (~24,000 to ~11,500 cal year BP). This interpretation corroborates existing pollen data indicating glacial-age savannah vegetation at CV (Smith et al., 2021), savannah and semi-deciduous dry forest communities at LCh (Burbridge et al., 2004), and C_4 dominated landscapes at HM (Maezumi et al., 2015; Figure 6). Similar glacial vegetation patterns of C_4 dominated landscapes have been documented at sites south of NKMNP in the Pantanal at Laguna La Gaiba (LLG; ~500 km southeast) (Whitney et al., 2011; Metcalfe et al., 2014) and Jaraguá cave (~850 km southeast of NKMNP) (Novello et al., 2019), suggesting the dominance of C_4 savannah grasslands during the last glacial period in the region. These data are consistent with previous modeling studies that simulate a replacement of rainforest with savannah/seasonally dry forest in ecotonal areas during the LGM (Beerling and Mayle, 2006).During the late glacial-Holocene transition, stable carbon isotope data indicate a progressive increase in C_3 vegetation (Figure 6) that corresponds with a period of poor pollen preservation at CV, an increase of semi-deciduous tropical dry forest at the expense of savannah vegetation at LCh after ~13,000 cal year BP, and a decrease in C_4 grass phytoliths at HM palm swamp after ~12,000 cal year BP (Figure 8), though it is likely that C_4 cerrado savannah persisted on the broader table mountain as a result of its rocky substrate and lack of soil (Mayle and Whitney, 2012; Maezumi et al., 2015). Model simulations demonstrate late glacial climate change (i.e., precipitation), drove the competitive replacement of drought-adapted vegetation (e.g., savannah or deciduous/semideciduous dry forest) by rainforest in drought-sensitive ecotonal areas (Beerling and Mayle, 2006). Precipitation increased in tropical lowland South America after ~12,800 cal year BP, as indicated by more frequent flooding and rising lake levels at LLG (Whitney et al., 2011), and in the Andes, water levels increased at Salar de Uyuni (Servant-Vildary et al., 2001) and Lake Titicaca (Baker et al., 2001). Reconstructions from LLG indicate that deglacial

temperatures in the lowland Bolivian Amazon rose by 4°C at 19,500 cal year BP and have likely remained relatively consistent until present (Whitney et al., 2011), supporting the interpretation that temperature was not the dominant driver of late glacial-Holocene vegetation change at NKMNP. It is important to note however, that temperature may not have been uniform across lowland Amazonia. For example, the presence of Podocarpaceae (*Podocarpus* sp.) at Lagoa da Curuça (0°46′S, 47°51′W) in the eastern Brazilian Amazon has been attributed to late glacial-Early Holocene cooling (Behling, 1996).

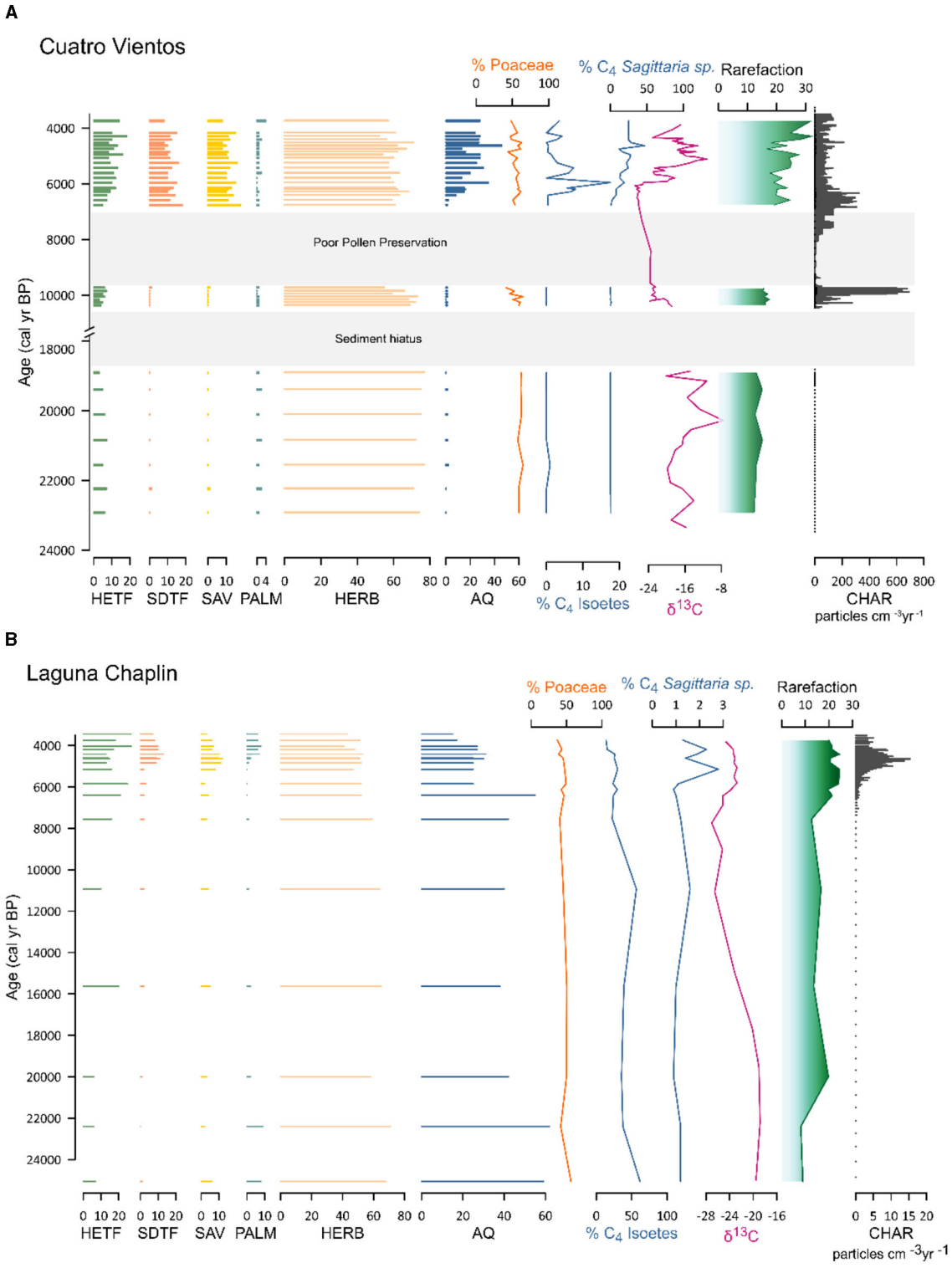

FIGURE 8 (Continued)

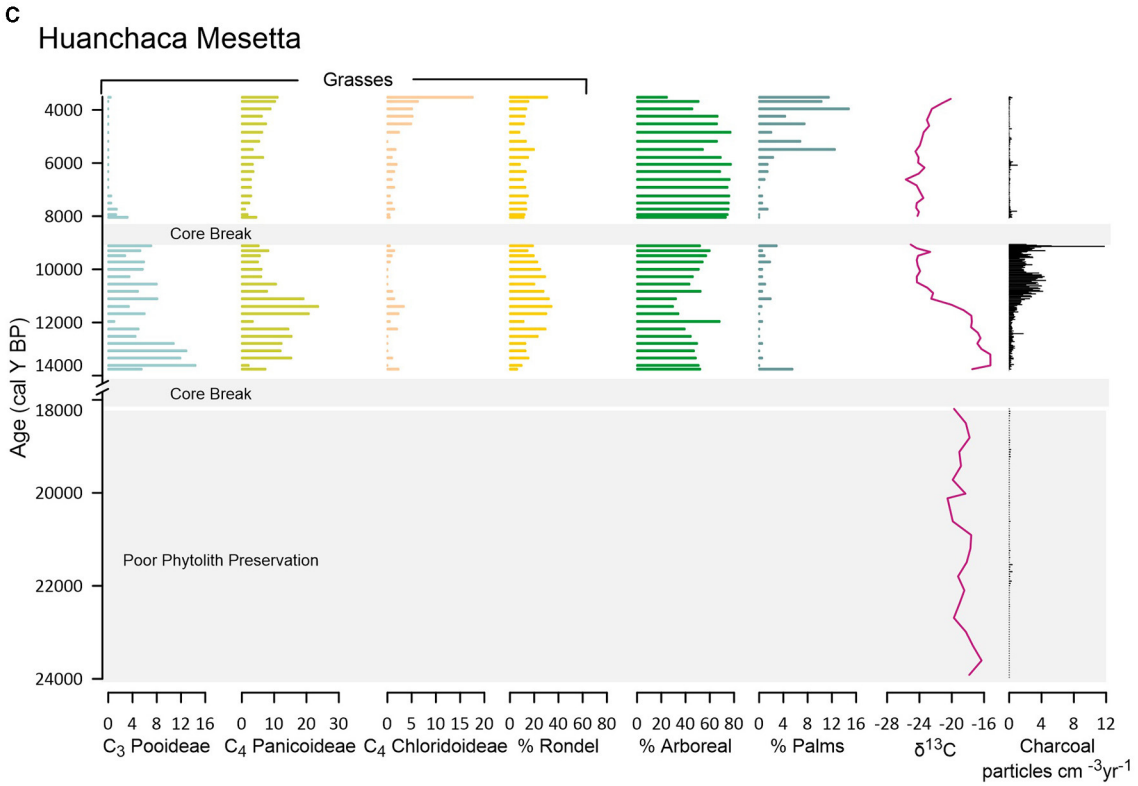

FIGURE 8 (Continued)
(A) Summarized vegetation from pollen, $\delta^{13}C$ and charcoal data for Cuatro Vientos: Humid evergreen tropical forest (HETF), Semi-deciduous tropical forest (SDTF), Savanna (SAV), palms (PALM), Herbaceous (HERB), Aquatics (AQ), percent Poaceae, % C_4 Isoetes, % C_4 Sagittatia sp., $\delta^{13}C$, Rarefaction, and charcoal accumulation (particles cm^{-3} $year^{-1}$). Y-axis broken from 18,000 to 11,000 cal year BP during sediment hiatus. **(B)** Summarized vegetation from pollen, $\delta^{13}C$ and charcoal data for Laguna Chaplin: Humid evergreen tropical forest (HETF), Semi-deciduous tropical forest (SDTF), Savanna (SAV), palms (PALM), Herbaceous (HERB), Aquatics (AQ), percent Poaceae, % C_4 Isoetes, % C_4 Sagittatia sp., $\delta^{13}C$, Rarefaction, and charcoal accumulation (particles cm^{-3} $year^{-1}$). **(C)** Summarized vegetation from phytoliths, $\delta^{13}C$ and charcoal data for Huanchaca Mesetta: Grasses: % C_3 Pooideae, % C_4 Panicoideae, % C_4 Chloridoideae, % Rondel, % Arboreal, % Palms, $\delta^{13}C$, and charcoal accumulation (particles cm^{-3} $year^{-1}$). Y-axis broken from 18,000 to 14,000 cal year BP during sediment hiatus.

The decline in drought-adapted C_4 vegetation associated with regionally wetter climates suggests that increased precipitation was likely the dominant driver shaping C_3-C_4 ARF-*Ecotone* vegetation dynamics in NKMNP during the glacial-interglacial transition. This interpretation is supported by palaeoecological studies from other drought-sensitive ecotonal areas around the Amazon Basin (Absy, 1991; Behling and Hooghiemstra, 1999; Sifeddine et al., 2001; Mayle et al., 2004). Interestingly, this interpretation contrasts with a recent record from Jaraguá cave (ca. 320 km east of NKMNP) that identified CO_2, opposed to temperature or precipitation, as the dominant driver of glacial-interglacial vegetation dynamics in western Brazil (Novello et al., 2019), demonstrating considerable spatial variability and the potential influence of different proxy data to determine drivers of late glacial vegetation responses in the tropical lowlands.

4.2 Documenting fire in C_4 Savannah grasslands during the last glacial period

During the LGP, minimal charcoal was present at NKMNP, however, determining the cause this absence of macrocharcoal is complicated by deposition and preservation issues associated with grass charcoal. Charcoal morphometrics based on aspect ratio can successfully differentiate woody and grass fuels (Vachula et al., 2021), however, previous studies document the overrepresentation of woody charcoal in grass dominated systems (Leys et al., 2015). To complicate this issue, recent charcoal dispersal models indicate that the dispersal of wood versus grass charcoal is not uniform, with fine grass charcoal particles being transported further than woody charcoal particles of the same size class (i.e., 125 μm) (Vachula and Rehn, 2023). Thus, the grass-charcoal component present in charcoal records from grass-dominated and mixed wood-grass ecosystems, such as NKMNP, likely represent broader regional fire histories than woody charcoal records from wood-dominated ecosystems. The pollen data at CV and LCh indicate the continued presence of woody fuels on the landscape during the LGP, thus if fire was present, we would anticipate woody charcoal to be present, if not overrepresented. In the absence of significant charcoal at any of the sites, we infer minimal LGP fire activity, across NKMNP.

The cooler glacial climate conditions and decreased evaporative moisture (Baker et al., 2001; Novello et al., 2019) in turn decreased the incidence of lightning-caused ignitions (Ramos-Neto and Pivello, 2000). The dominance of C_4 grasses would have reduced fuel loads and decreased fuel connectivity (Cochrane and Ryan, 2009). Coupled with the lower incidence of lightning-caused

10.3389/fearc.2023.1208985

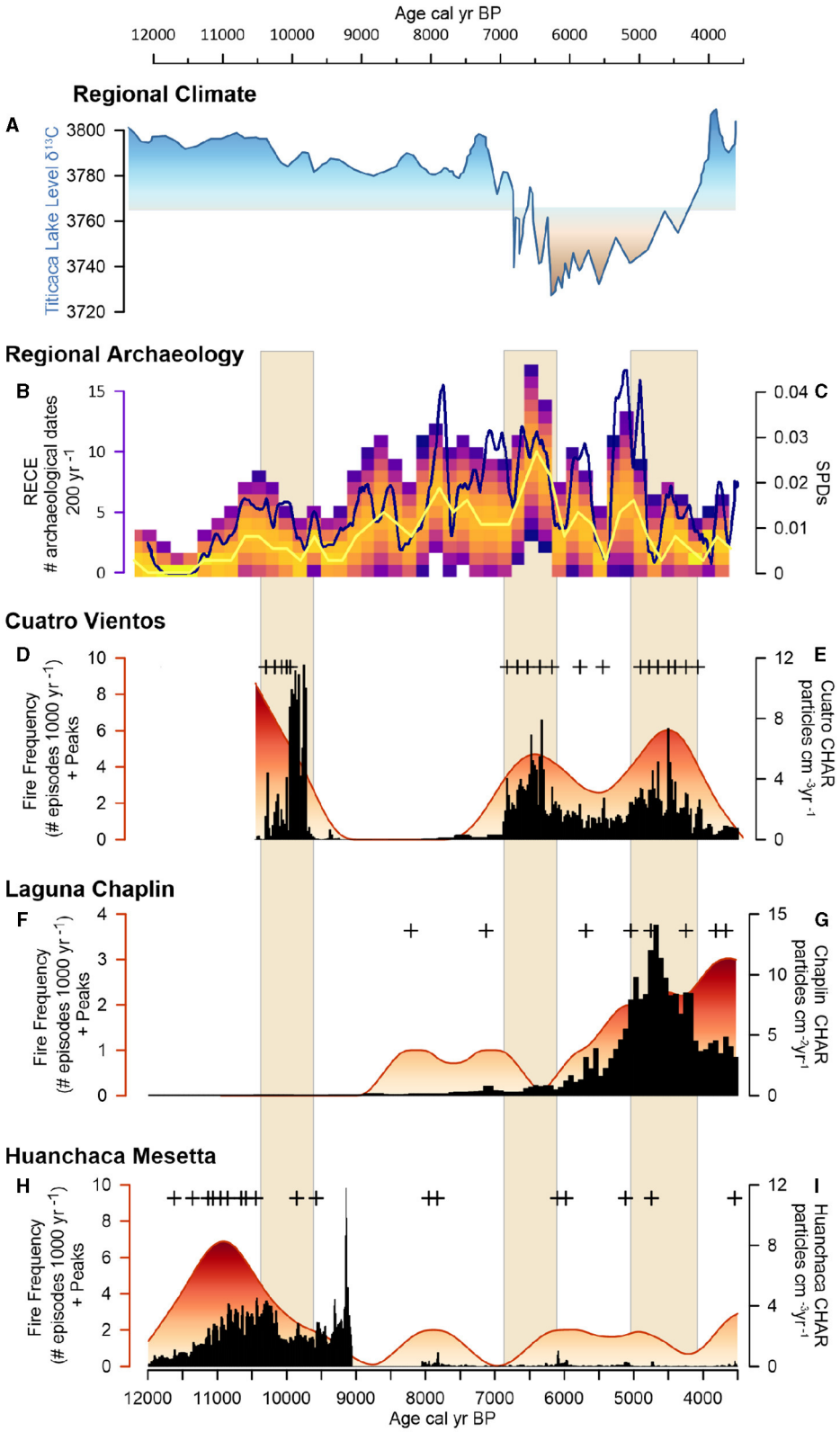

FIGURE 9
Climate, humans and fire activity: **(A)** Regional palaeoclimate record from Lake Titicaca $\delta^{13}C$ (PDB) (Baker et al., 2001), **(B)** RECE model and **(C)** SPD curve from regional radiocarbon dates (Supplementary Table S4), **(D)** Cuatro Vientos (CV) fire frequency: red fill, fire peak: plus sign, **(E)** CV Charcoal accumulation (CHAR): black line, **(F)** Laguna Chaplin (LCh) fire frequency: red fill, fire peak: plus sign, **(G)** LCh charcoal accumulation: black line, **(H)** Huanchaca Mesetta (HM) re frequency: red fill, fire peak: plus sign, **(I)** HM charcoal accumulation.

fires, these factors likely contributed to decreased fire activity in NKMNP during the LGP. Previous research suggests that ecological disturbance by fire is a fundamental component of C_4 grassland ecosystems (Keeley and Rundel, 2005; Beerling and Osborn, 2006; Edwards et al., 2010) and demonstrates that fire was an essential feedback mechanism leading to C_4 grassland expansion during the late Miocene (8–3 MYA) (Edwards et al., 2010; Strömberg, 2011; Bouchenak-Khelladi et al., 2014; Kirschner and Hoorn, 2019). Additionally, studies from the southwestern African grasslands of Namibia demonstrate that intensified fire activity caused by aridification triggered the initial establishment and later dominance of C_4 plants (Hoetzel et al., 2013). Although the presence of fire activity may have been essential in the initial evolution and establishment of C_4 grassland ecosystems, the absence of fire activity in our study sites during the LGM suggests that fire was not necessary for the presence and maintenance of C_4 savannah grasslands in NKMNP for over 24,000 years. These data challenge recent model simulations that indicate fire and low CO_2 were responsible for the expansion of the savannah vegetation in the southern ecotone margins of the Amazon during the LGM (Sato et al., 2021). Alternatively, our data support previous interpretations that low LGM CO_2 values and drier conditions likely helped to maintain the C_4 dominated system in NKMNP (Burbridge et al., 2004).

4.3 The influence of basin size in recording fire and vegetation dynamics in the ARF-ecotone

The glacial-Holocene transition (ca. 13,500–10,000 cal year BP) was characterized by a shift toward wetter conditions after 12,800 cal year BP in tropical lowland South America, coupled with oscillating periods of dry and wet conditions (Baker et al., 2001; Whitney et al., 2011; Novello et al., 2017). Despite increased precipitation variability, stable carbon isotope data indicate a progressive replacement of C_4 savannah grasslands with C_3 woody vegetation at our study sites (Figure 8). The stable isotope data corroborate existing pollen records indicating increased woody vegetation at CV and LCh (Burbridge et al., 2004; Maezumi et al., 2015) and decreasing C_4 phytoliths within the HM palm swamp (Maezumi et al., 2015). There was an increase in macrocharcoal values at HM ~12,000 to 9,000 cal year BP and at CV between 10,500 to 9,600 cal year BP.

The transition from cool-dry glacial climates to warm-wet climates in the early Holocene likely increased the incidence of convective thunder storms and lightning-induced fires at HM. Empirical studies of fire activity in the Emas National Park, Brazil (~900 km southeast of NKMNP) indicate that the majority of modern fires in the cerrado savannahs occur during the wet season (October–April), with a significantly higher occurrence of lightning-caused fires in open vegetation (wet field or grassy savannahs) on flat plateau areas, similar to the table mountain in NKMNP (Ramos-Neto and Pivello, 2000). Over a four-year period (1995–1999), wet season lightning fires were frequent ($n = 31$ fires burning ~30,000 ha), patchy, and extinguished by rain, likely representing the natural fire regime in the region (Ramos-Neto and Pivello, 2000). These data support the interpretation that HM likely represents the natural lightning-induced fire regime since the LGM.

Below the table mountain at CV, wetter climate conditions after 12,800 cal year BP (Whitney et al., 2011) likely increased fuel accumulation, fuel connectivity, and fuel moisture. The later may have made it more difficult for lightning-ignited fires to spread. LCh does not record an increase in fire activity during this period (Figure 9), despite similar declines in C_4 to vegetation indicated by the decrease in $\delta^{13}C$ (from −16 to −24‰) and C/N values (>12; Figures 6, 7). The synchronicity of fire activity at the smaller lake basins of CV and HM, but not the larger lake basin of LCh, suggests basin size may have influenced the detection of fire activity between the records. In most forested ecosystems, macrocharcoal deposition typically occurs within 1 km of the lake (Clark et al., 1998; Lynch et al., 2004; Oris et al., 2014). However, in open grasslands in the South African Savannah, Afrotropics and North American tall-grass prairies, macrocharcoal deposition typically occurs within 5 km of the lake (Duffin et al., 2008; Aleman et al., 2013; Leys et al., 2015), though recent charcoal dispersal models suggest fine grass charcoal particles may be transported further (Vachula and Rehn, 2023). The close proximity of CV to LCh (<6 km) suggests these study sites should have similar fire histories. However, additional palaeoecological studies indicate small lake basins (<5 km^2) are more sensitive to detecting local-scale (1–10^6 m^2) fire activity, while large sedimentary basins (>50 km^2) capture regional (>10^{10} m^2) macrocharcoal signals (Power et al., 2010). The presence of fire activity recorded in the small basins of CV and HM, but not the large basin of LCh, suggests these small basins are likely more sensitive to detecting local-scale fire activity (i.e. slash and burn cultivation fires) in the ARF-*Ecotone*. This interpretation corroborates existing studies documenting the influence of basin size on fire detection sensitivity in lake sediment basins ~300 km north of NKMNP (Carson et al., 2014).

4.4 Fire and human linkages during the early to middle Holocene (11,000–3,700 cal year BP)

In addition to basin size, the increase in the spatial variability of fire after 10,500 cal year BP at CV and LCh raises the possibility that climate (i.e., lightning) was not the dominant cause of ignitions. Previous studies have shown that increased spatial variability of fire, despite similar vegetation and climate, may be attributed to increased human influence (Bush et al., 2007a; Mayle and Power, 2008; Marlon et al., 2013; Maezumi et al., 2018b). A large spike in macrocharcoal has been documented at numerous sites in the Amazonian lowlands when areas were first occupied by humans (Bush et al., 2007a, 2016). Recent studies demonstrate that the ARF-*Ecotone* was extensively occupied since the early Holocene (after 10,500 cal year BP) with thousands of human-managed artificial forest islands documented across the Llanos de Moxos plains (~350 km west of NKMP) (Lombardo et al., 2013, 2020; Capriles et al., 2019). Additionally, recent distribution models estimate between 10,000 and 24,000 sites remain to be discovered in the region (Peripato et al., 2023).

The ARF-*Ecotone* region was also a center for early Holocene plant domestication (Oliver, 2008; Clement et al., 2010, 2015; de Cristo-Araújo et al., 2013; Brugger et al., 2016; Hilbert et al., 2017; Kistler et al., 2018; Watling et al., 2018; Lombardo et al., 2020). Cultivating crops (i.e., maize, manioc, sweet potato, squash, arrow root) was often coupled with Indigenous burning (Brugger et al., 2016; Bush et al., 2016; Maezumi et al., 2018b, 2022; Iriarte et al., 2020). Maize and Indigenous burning has been well-documented in the region in the anthropic forest islands [∼6,850 cal year BP; (Lombardo et al., 2020)], Lake Rogaguado [∼6,500 cal year BP; (Brugger et al., 2016)], Lake Versalles [∼5,700 cal year BP; (Maezumi et al., 2022), and the Monte Castelo shell-mound [∼5,300 cal year BP (Hilbert et al., 2017; Furquim et al., 2021)]. Previous palaeoecological studies demonstrate that crop cultivation was not uniform across the landscape; while some Amazon lake records had limited evidence of cultivation and fire activity, neighboring lakes with similar basin characteristics (<50 km away) had histories of crop cultivation and fire activity for millennia (Burbridge et al., 2004; Bush et al., 2007a,b; Carson et al., 2014; Brugger et al., 2016; McMichael and Bush, 2019). This may account for the spatial variability of fire and presence of maize cultivation at LCh (Maezumi et al., 2018b) but not at CV.

Another compelling line of evidence documenting the prevalence of past Indigenous burning comes from Amazonian Dark Earth Soils (ADEs). ADEs are human made soils that have high charcoal concentrations and organic matter, higher pH values and greater concentrations of P, Ca, and Mg which enable them to maintain nutrient levels over hundreds of years (Lehmann et al., 2003; Glaser and Woods, 2004; Woods et al., 2009). The earliest ADEs are documented in the Upper Madeira ∼6,000 years ago (Mora et al., 1991; Watling et al., 2018), at the Teotônio site (ca. 600 km NW of NKMNP) where crops such as Cucurbita (squash) and Phaseolus (beans) were grown (Watling et al., 2018). While the widespread formation of ADEs across the Amazon did not begin until after the termination of the CV record ∼2,500 cal year BP (Iriarte et al., 2020), the incipient land use practices trace their origins to the early to middle Holocene.

Archaeological studies have also identified the importance of riverine bluff habitats for Indigenous settlement, ADE soil formation, crop cultivation, and migration corridors (Denevan, 1996, 2005; Heckenberger et al., 2008; McMichael et al., 2014). The close proximity of CV to the Rio Paraguá (Figure 1) would have made it an optimal location for Indigenous utilization of the naturally open, mosaic landscape in the early Holocene (Figure 10). At CV there was a significant increase in macrocharcoal values at CV ∼6,500 to 6,000 cal year BP that was not documented at LCh despite similar savannah-SDTF mosaic vegetation at both sites. The spatial variability of fire coupled with the synchronous increase in human activity in the region indicated by the SPD and RECE values (Figure 9), may be attributed to increased human-caused ignitions at this time. Climate likely also promoted fire by decreasing fuel moisture and increasing flammability during the MHDP, that would have in turn promoted natural fires (Bowman et al., 2009) and made Indigenous burning a more effective tool for land management (Mayle and Power, 2008; Bowman et al., 2020). However, while it is possible that humans have been influencing fire activity in NKMNP since the early Holocene (∼10,500 cal year BP), additional archaeological evidence is needed to support this interpretation.

4.5 Climate and vegetation linkages during the mid-Holocene dry period (6,000–4,000 cal year BP)

The MHDP was characterized by significantly drier-than-present climate conditions with longer, more extreme dry seasons across much of tropical South America (Baker et al., 2001; Wang et al., 2007; Mayle and Whitney, 2012; Cheng et al., 2013; Kanner et al., 2013; Bernal et al., 2016). The MHDP has been attributed to lower southern-hemispheric summer insolation levels driven by the precessional cycle of Earth's orbit (Berger and Loutre, 1991). This restricted the southerly migration of the ITCZ (Haug et al., 2001) and decreased the strength of the SASM (Cruz et al., 2009; Baker and Fritz, 2015; Novello et al., 2017). The CV and LCh pollen records (Burbridge et al., 2004; Smith et al., 2021) and the phytolith record from HM (Maezumi et al., 2015) indicate a savannah-SDTF mosaic dominated the NKMNP landscape during the MHDP. Around 7,000 cal year BP higher $\delta^{13}C$ values at CV correspond to an increase in aquatic/semi-aquatic macrophytes *Sagittaria* (∼30%−40%) and *Isoetes* (∼10%), indicating a shift from a clear open lake to a shallower more eutrophic environment (Smith et al., 2021). The dry conditions of the MHDP likely lowered lake levels creating optimal conditions for *Sagittaria* which grows in shallow waters (15–30 cm deep) along lake shores and requires exposed mud for successful seedling establishment (Jepson, 1993). Higher levels of %N (3–5; Figure 5) indicates increased nitrogen fixation, likely from the increase in *Sagittaria* which has high rates of N_2 fixation (Arima and Yoshida, 1982) and lower $\delta^{15}N$ values (−2‰). At LCh the mid-Holocene expansion of *Isoetes* was also attributed to shallower conditions that allowed this aquatic plant to spread from the lake shore-line across the lake (Burbridge et al., 2004). The increased abundance of these aquatic macrophytes at CV and LCh was coupled with consistent levels of Poaceae (∼50%) at both sites, suggesting C_4 grass was not the dominant driver of the $\delta^{13}C$ values during this period. Some aquatic plants, such as *Sagittaria* (Sage, 2004), predominantly utilize the C_4 photosynthetic pathway ($\delta^{13}C$ −12 to −13‰) (Ehleringer et al., 1991), while *Isoetes* uses the CAM photosynthetic pathway which can have a similar $\delta^{13}C$ value (range −20 to −10‰) to C_4 plants (O'Leary, 1988). Together, the increase in *Sagittaria* and *Isoetes,* as a result of lower lake levels, likely drove the increased $\delta^{13}C$ values at CV and LCh during the MHDP (Figure 10).

Additional evidence of vegetation response to regional drying has been documented in the Llanos de Moxos, where seasonally flooded savannahs were replaced by dry cerrado savannah vegetation (Mayle et al., 2007; Lombardo et al., 2019). The longer and more severe dry seasons were associated with a decrease in seasonal flooding during the MHDP (Mayle and Power, 2008), increased available land for cultivation and enabled the expansion of C_3 tree populations, intolerant of waterlogging, into the low-lying plains of the Llanos de Moxos (Mayle et al., 2007; Lombardo et al., 2019).

10.3389/fearc.2023.1208985

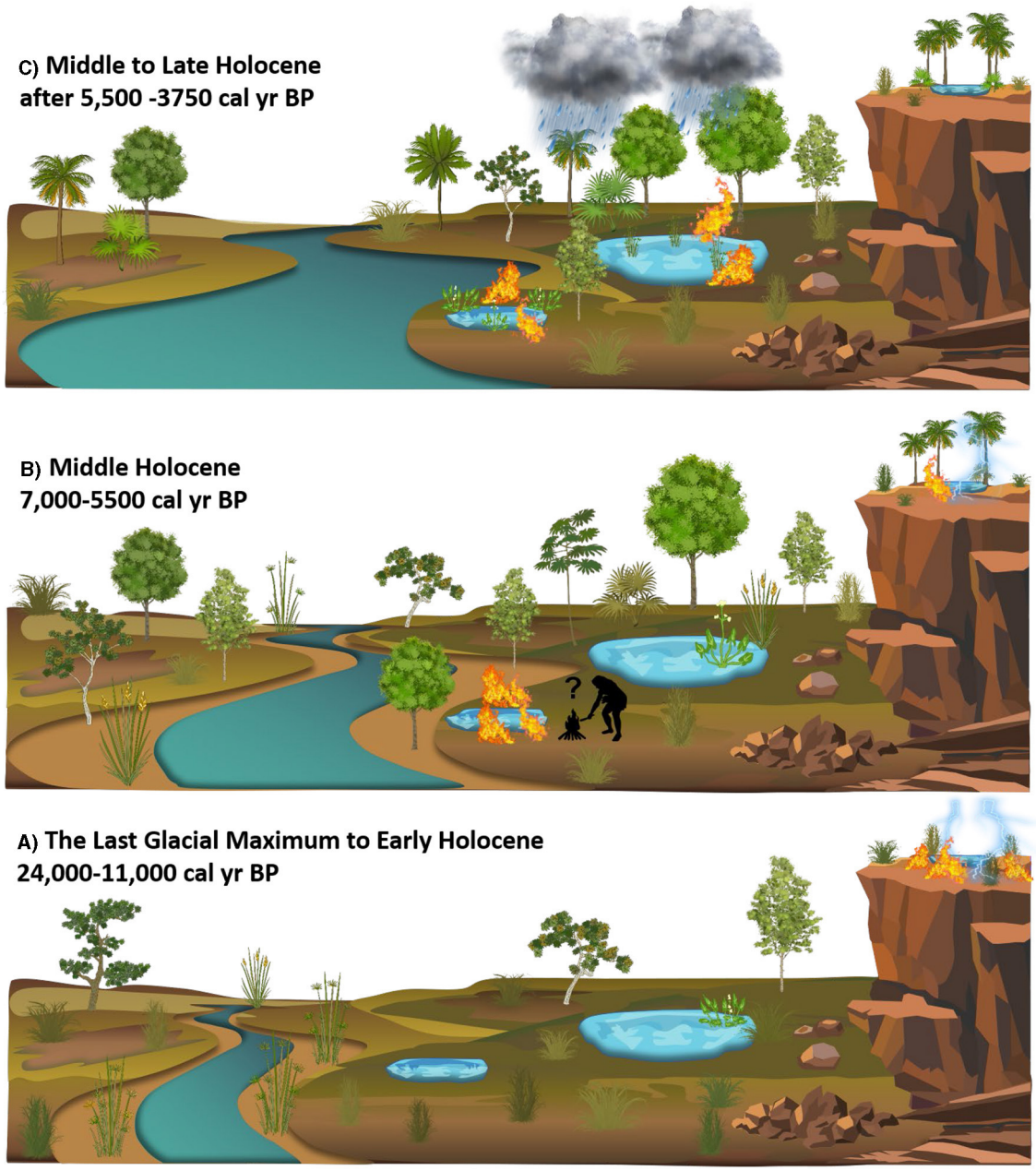

FIGURE 10
A conceptual figure of the landscape change since the Last Glacial Maximum in Northeast Bolivia. **(A)** End of the Last Glacial 24,000–11,000 cal year BP characterized by open seasonally flooded savannah taxa including Poaceae, Cyperaceae, Betulaceae (*Alnus*), Aquifoliaceae (*Ilex),* Podocarpaceae, and *Paullinia*/*Roupala*, with low concentration of *Curatella americana*, **(B)** Middle Holocene 7,000–5,500 cal year BP characterized by *Anadenanthera*, *Astronium Curatella americana* Poaceae, *Sagittaria,* and *Isoetes*, **(C)** Middle to Late Holocene 5,500–3,750 cal year BP characterized by Moraceae/Urticaceae, *Mauritia*/*Mauritiella* palms, and increased *Sagittaria,* and *Isoetes*.

4.6 Fire activity and pollen species richness in the middle Holocene (7,000–3,700 cal year BP)

After ca. 5,000 cal year BP the spatial variability of fire in NKMNP begins to decrease, as indicated by similar macrocharcoal signatures at CV and LCh. The similarity in the macrocharcoal records suggest climate was likely the dominant driver of the regional increase in fire at CV, however, as humans are present in the region surrounding NKMNP (Figure 9), human-caused ignitions should not be ruled out and future archaeological research within the park may help to resolve this issue.

Interestingly, there is a slight negative correlation between fire activity and pollen species richness (Figure 8) at CV and LCh during this time that is likely attributed to declines in non-fire tolerant rainforest taxa (e.g., Moraceae/Urticaceae) immediately

following a period of increased fire activity. However, at both CV and LCh, pollen diversity levels return to, or exceed pre-fire levels, suggesting that fire did not have a long-lasting negative influence on pollen species richness. Ethnographic studies have shown that through agroforestry practices (Denevan, 2006; Levis et al., 2018), even small groups of hunter-gatherers can change the configuration of useful plant species and create more productive environments surrounding human settlements (Posey and Balée, 1989; Politis, 1996; Denevan, 2006; Levis et al., 2018). For example agroforestry and Indigenous burning can increase alpha (local) and beta (regional) biodiversity in anthropogenic forests (Balée, 2000; Junqueira et al., 2010; Neves, 2012; ter Steege et al., 2013; Clement et al., 2015; Lins et al., 2015; Arroyo-Kalin, 2018). These studies, combined with the potential influence of Indigenous burning throughout the Holocene, raise the intriguing possibility that the composition of modern flora at NKMNP developed as part of a co-evolutionary process between people and plants that started at the beginning of its occupation as proposed in other sites in the Amazon (Furquim et al., 2023).

Fire activity decreases at CV and LCh after 4,500 cal year BP, likely as a result of the progressive increase in precipitation associated with the end of the MHDP (Mayle et al., 2000; Baker et al., 2001; Wang et al., 2007; Mayle and Whitney, 2012; Cheng et al., 2013; Kanner et al., 2013; Bernal et al., 2016; Lombardo et al., 2018) in response to the strengthening of the SASM driven by gradually increasing insolation levels (Berger and Loutre, 1991; Cruz et al., 2005; Baker and Fritz, 2015). This resulted in local seasonal flooding at CV and the establishment of *M. flexuosa* consistent with regional records indicating the expansion of both riverine and *terra firme* tropical rainforest (Mayle et al., 2000; Carson et al., 2014; Brugger et al., 2016). Unfortunately, the CV record terminates at 3750 cal year BP prior to the establishment of the modern palm swamp and the apex of regional human activity in the region (Heckenberger and Neves, 2009; Maezumi et al., 2018b; de Souza et al., 2019; Arroyo-Kalin and Riris, 2021).

5 Conclusions

This study reconstructs vegetation and palaeofire activity in the Bolivian ARF-*Ecotone* for the past 24,000 years (i.e., from the LGM to the late Holocene). Our data indicate that C_4 terrestrial savannah vegetation dominated the CV, LCh, and HM catchments during the glacial-Holocene transition. Additionally, fire was likely not a requisite for the maintenance of C_4 savannah-woodland ecosystems during the late glacial Period. The influence of basin size on the detection of palaeofire activity compliments existing pollen studies indicating the greater sensitivity of small lake basins to detect local-scale fire activity, supporting our hypothesis. Increased spatial variability of fire coupled with continuous presence of human occupation and regional maize cultivation suggests that humans may have contributed to the increased heterogeneity of fire at NKMNP during the Holocene. The close proximity of CV to the Rio Paragua would have made it an ideal settlement location for Indigenous occupation (likely less so once it became a swamp after ~3,750 cal year BP); however, archaeological surveys and excavations in the NKMNP area are still needed. While pollen richness declined with peak fire activity, richness values recovered to equivalent or higher levels following fire events, suggesting that the increase in fire at CV and LCh during the Holocene did not have a lasting negative influence on savannah-SDTF vegetation at NKMNP. While NKMNP has long been celebrated for its "pristine" ecosystems, the data presented here add to the increasing body of evidence that Indigenous peoples may have had a long, multi-millennial history of managing Bolivian Amazon ecosystems through fire and agroforestry. Hence, it is increasingly likely that, through millennia of land use, humans may have helped shape patterns of biodiversity in NKMNP, that potentially has a strong legacy in today's forests. Incorporating insights from Indigenous traditional ecological knowledge may contribute useful insights in combining biodiversity conservation and maintenance of ecosystem services with sustainable land use.

Data availability statement

The original contributions presented in the study are included in the article/Supplementary material, further inquiries can be directed to the corresponding author.

Author contributions

Conceptualization: SM, MP, KM, and FM. Methodology, resources, project administration, and funding acquisition: SM, MP, and FM. Fieldwork and sample collection: FM. Formal analysis, data curation, writing—original draft preparation, and visualization: SM. Writing—review and editing: SM, RS, MP, AK, PR, CC, KM, and FM. Supervision: MP and FM. All authors contributed to the article and approved the submitted version.

Funding

Funding for this research was provided to SM by Global Change and Sustainability Center, the Graduate Research Fellowship, the Don Currey Graduate Research Fellowship, and the PAGES Graduate Research Fellowship. The University of Leicester provided a start-up grant to FM (1995) to support the fieldwork. SM and PR would like to thank the Max Planck Society for funding.

Acknowledgments

We thank Mary McIntyre and Daniel Harris for their help in sample preparation and analysis. We thank Dr. Tim Killeen and the Museo de Historia Natural Noel Kempff Mercado, Santa Cruz, Bolivia for providing logistical support, and in particular Rene Guillen and local guides from the village of Florida (e.g., Juan Surubi) for assistance with accessing the site, coring the

site, and plant identification. We also thank the two reviewers for their critical reading and suggested improvements to help clarify our manuscript.

Conflict of interest

The authors declare that the research was conducted in the absence of any commercial or financial relationships that could be construed as a potential conflict of interest.

The handling editor GS declared a past collaboration with the author(s).

The author(s) AB, PR declared that they were an editorial board member of Frontiers, at the time of submission. This had no impact on the peer review process and the final decision.

Publisher's note

Supplementary material

The Supplementary Material for this article can be found online at: https://www.frontiersin.org/articles/10.3389/fearc.2023.1208985/full#supplementary-material

References

Absy, M. (1991). Occurrence of four episodes of rain forest regression in southeastern Amazonia during the last 60 000 yrs. First comparison with other tropical regions [Mise en evidence de quatre phases d'ouverture de la foret dense dans le sud-est de l'Amazonie au cours. *C. R. Acad. Sci. Ser. II.* 312, 673–678.

Aleman, J. C., Blarquez, O., Bentaleb, I., Bont,é, P., Brossier, B., Carcaillet, C., et al. (2013). Tracking land-cover changes with sedimentary charcoal in the Afrotropics. *Holocene* 23, 1853–1862. doi: 10.1177/0959683613508159

Ambrose, S. H., and Sikes, N. E. (1991). Soil carbon isotope evidence for holocene habitat change in the kenya rift valley. *Science* 253, 1402–1405. doi: 10.1126/science.253.5026.1402

Aranibar, J. N., Anderson, I. C., Epstein, H. E., Feral, C. J. W., Swap, R. J., Ramontsho, J., et al. (2008). Nitrogen isotope composition of soils, C3 and C4 plants along land use gradients in southern Africa. *J. Arid Environ.* 72, 326–337. doi: 10.1016/j.jaridenv.2007.06.007

Arima, Y., and Yoshida, T. (1982). Nitrogen fixation and denitrification in the roots of flooded crops. *Soil Sci. Plant Nutr.* 28, 483–489. doi: 10.1080/00380768.1982.10432388

Arroyo-Kalin, M. (2018). Human Niche construction and population growth in pre-Columbian Amazonia. *Archaeol. Int.* 20, 122–136. doi: 10.5334/ai-367

Arroyo-Kalin, M., and Riris, P. (2021). Did pre-Columbian populations of the Amazonian biome reach carrying capacity during the Late Holocene? *Philos. Trans. R. Soc. Lond. B Biol. Sci.* 376, 20190715. doi: 10.1098/rstb.2019.0715

Baker, P. A., and Fritz, S. C. (2015). Nature and causes of Quaternary climate variation of tropical South America. *Quat. Sci. Rev.* 124, 31–47. doi: 10.1016/j.quascirev.2015.06.011

Baker, P. A., Seltzer, G. O., Fritz, S. C., Dunbar, R. B., Grove, M. J., Tapia, P. M., et al. (2001). The history of South American tropical precipitation for the past 25,000 years. *Science* 291, 640–643. doi: 10.1126/science.291.5504.640

Balée, W. (2000). Antiquity of traditional ethnobiological knowledge in Amazonia: the Tupí-Guaraní family and time. *Ethnohistory* 47, 399–422. doi: 10.1215/00141801-47-2-399

Barreto, C., Lima, H. P., and Betancourt, C. J. (2016). *Cerâmicas Arqueológicas da Amazônia: Rumo a Uma Nova Síntese*. Belém: IPHAN, Museu Paraense Emílio Goeldi.

Beerling, D. J., and Mayle, F. E. (2006). Contrasting effects of climate and CO_2 on Amazonian ecosystems since the last glacial maximum. *Glob. Chang. Biol.* 12, 1977–1984. doi: 10.1111/j.1365-2486.2006.01228.x

Beerling, D. J., and Osborn, C. P. (2006). The origin of the savanna biome. *Glob. Chang. Biol.* 12, 2023–2031. doi: 10.1111/j.1365-2486.2006.01239.x

Behling, H. (1996). First report on new evidence for the occurrence of Podocarpus and possible human presence at the mouth of the Amazon during the Late-glacial. *Veget. Hist. Archaebot.* 5, 241–246. doi: 10.1007/BF00217501

Behling, H., and Hooghiemstra, H. (1999). Environmental history of the Colombian savannas of the Llanos Orientales since the Last Glacial Maximum from lake records El Pinal and Carimagua. *J. Paleolimnol.* 21, 461–476. doi: 10.1023/A:1008051720473

Berger, A., and Loutre, M. F. (1991). Insolation values for the climate of the last 10 million years. *Quat. Sci. Rev.* 10, 297–317. doi: 10.1016/0277-3791(91)90033-Q

Bernal, J. P., Cruz, F. W., Stríkis, N. M., Wang, X., Deininger, M., Catunda, M. C. A., et al. (2016). High-resolution Holocene South American monsoon history recorded by a speleothem from Botuverá Cave, Brazil. *Earth Planet. Sci. Lett.* 450, 186–196. doi: 10.1016/j.epsl.2016.06.008

Bevan, A., Colledge, S., Fuller, D., Fyfe, R., Shennan, S., and Stevens, C. (2017). Holocene fluctuations in human population demonstrate repeated links to food production and climate. *Proc. Natl. Acad. Sci. USA.* 114, E10524–E10531. doi: 10.1073/pnas.1709190114

Birks, H. J. B., and Line, J. M. (1992). The use of rarefaction analysis for estimating palynological richness from Quaternary pollen-analytical data. *Holocene* 2, 1–10. doi: 10.1177/095968369200200101

Blaauw, M., and Christen, J. A. (2011). Flexible palaeoclimate age-depth models using an autoregresive gamma process. *Bayesian Anal.* 6, 457–474. doi: 10.1214/ba/1339616472

Blaauw, M., Christen, J. A., Bennett, K. D., and Reimer, P. J. (2018). Double the dates and go for Bayes—impacts of model choice, dating density and quality on chronologies. *Quat. Sci. Rev.* 188, 58–66. doi: 10.1016/j.quascirev.2018.03.032

Boivin, N. L., Zeder, M. A., Fuller, D. Q., Crowther, A., Larson, G., Erlandson, J. M., et al. (2016). Ecological consequences of human niche construction: examining long-term anthropogenic shaping of global species distributions. *Proc. Nat. Acad. Sci.* 113, 6388–6396. doi: 10.1073/pnas.1525200113

Bond, W. J., Stock, W. D., and Hoffman, M. T. (1994). Has the Karoo spread? A test for desertification using carbon isotopes from soils. *S. Afr. J. Sci.* 90, 391–397.

Bouchenak-Khelladi, Y., Slingsby, J. A., Verboom, G. A., and Bond, W. J. (2014). Diversification of C(4) grasses (Poaceae) does not coincide with their ecological dominance. *Am. J. Bot.* 101, 300–307. doi: 10.3732/ajb.1300439

Bowman, D. M. J. S., Balch, J. K., Artaxo, P., Bond, W. J., Carlson, J. M., Cochrane, M., et al. (2009). Fire in the earth system. *Science* 324, 481–484. doi: 10.1126/science.1163886

Bowman, D. M. J. S., Kolden, C. A., Abatzoglou, J. T., Johnston, F. H., van der Werf, G. R., and Flannigan, M. (2020). Vegetation fires in the Anthropocene. *Nat. Rev. Earth Environ.* 1, 500–515. doi: 10.1038/s43017-020-0085-3

Bowman, D. M. J. S., Perry, G. L. W., Higgins, S. I., Johnson, C. N., Fuhlendorf, S. D., and Murphy, B. P. (2016). Pyrodiversity is the coupling of biodiversity and fire regimes in food webs. *Philos. Trans. R. Soc. Lond. B Biol. Sci.* 371, 20150169. doi: 10.1098/rstb.2015.0169

Brando, P., Macedo, M., Silvério, D., Rattis, L., Paolucci, L., Alencar, A., et al. (2020). Amazon wildfires: scenes from a foreseeable disaster. *Flora* 268, 151609. doi: 10.1016/j.flora.2020.151609

Brando, P. M., Silvério, D., Maracahipes-Santos, L., Oliveira-Santos, C., Levick, S. R., Coe, M. T., et al. (2019). Prolonged tropical forest degradation due to compounding disturbances: implications for CO_2 and H_2O fluxes. *Glob. Chang. Biol.* 25, 2855–2868. doi: 10.1111/gcb.14659

Brugger, S. O., Gobet, E., van Leeuwen, J. F. N., Ledru, M.-P., Colombaroli, D., van der Knaap, W. O., et al. (2016). Long-term man–environment interactions in the Bolivian Amazon: 8000 years of vegetation dynamics. *Quat. Sci. Rev.* 132, 114–128. doi: 10.1016/j.quascirev.2015.11.001

Burbridge, R. E., Mayle, F. E., and Killeen, T. J. (2004). Fifty-thousand-year vegetation and climate history of Noel Kempff Mercado National Park, Bolivian Amazon. *Quat. Res.* 61, 215–230. doi: 10.1016/j.yqres.2003.12.004

Bush, M. B., Correa-Metrio, A., McMichael, C. H., Sully, S., Shadik, C. R., Valencia, B. G., et al. (2016). A 6900-year history of landscape modification by humans in lowland Amazonia. *Quat. Sci. Rev.* 141, 52–64. doi: 10.1016/j.quascirev.2016.03.022

Bush, M. B., McMichael, C. H., Piperno, D. R., Silman, M. R., Barlow, J., Peres, C. A., et al. (2015). Anthropogenic influence on Amazonian forests in pre-history: an ecological perspective. *J. Biogeogr.* 42, 2277–2288. doi: 10.1111/jbi.12638

Bush, M. B., and Silman, M. R. (2004). Observations on Late Pleistocene cooling and precipitation in the lowland Neotropics. *J. Quat. Sci.* 19, 677–684. doi: 10.1002/jqs.883

Bush, M. B., Silman, M. R., de Toledo, M. B., Listopad, C., Gosling, W. D., Williams, C., et al. (2007a). Holocene fire and occupation in Amazonia: records from two lake districts. *Philos. Trans. R. Soc. Lond. B Biol. Sci.* 362, 209–218. doi: 10.1098/rstb.2006.1980

Bush, M. B., Silman, M. R., and Listopad, C. M. C. S. (2007b). A regional study of Holocene climate change and human occupation in Peruvian Amazonia. *J. Biogeogr.* 34, 1342–1356. doi: 10.1111/j.1365-2699.2007.01704.x

Capriles, J. M. (2023). A review of archaeological and paleoecological radiocarbon dating in Bolivia. *Open Quat.* 9, 2. doi: 10.5334/oq.118

Capriles, J. M., Lombardo, U., Maley, B., Zuna, C., Veit, H., and Kennett, D. J. (2019). Persistent early to middle Holocene tropical foraging in southwestern Amazonia. *Sci. Adv.* 5, eaav5449. doi: 10.1126/sciadv.aav5449

Carleton, W. C. (2021). Evaluating Bayesian radiocarbon-dated event count (REC) models for the study of long-term human and environmental processes. *J. Quat. Sci.* 36, 110–123. doi: 10.1002/jqs.3256

Carleton, W. C., and Groucutt, H. S. (2021). Sum things are not what they seem: problems with point-wise interpretations and quantitative analyses of proxies based on aggregated radiocarbon dates. *Holocene* 31, 630–643. doi: 10.1177/0959683620981700

Carson, J. (2014). *Pre-Columbian Land Use and Human Impact in the Bolivian Amazon*. Edinburgh: University of Edinburgh.

Carson, J. F., Watling, J., Mayle, F. E., Whitney, B. S., Iriarte, J., Prümers, H., et al. (2015). Pre-Columbian land use in the ring-ditch region of the Bolivian Amazon. *Holocene* 25, 1285–1300. doi: 10.1177/0959683615581204

Carson, J. F., Whitney, B. S., Mayle, F. E., Iriarte, J., Prümers, H., Soto, J. D., et al. (2014). Environmental impact of geometric earthwork construction in pre-Columbian Amazonia. *Proc. Natl. Acad. Sci. USA.* 111, 1–6. doi: 10.1073/pnas.1321770111

Centro de Previsão de Tempo e Estudos Climáticos, Instituto Nacional de Pesquisas da Amazônia [CPTEC/INPA] (2023). Available online at: https://www.cptec.inpe.br/ (accessed October 12, 2023).

Cerling, T. E. (1984). The stable isotopic composition of modern soil carbonate and its relationship to climate. *Earth Planet. Sci. Lett.* 71, 229–240. doi: 10.1016/0012-821X(84)90089-X

Cheng, H., Sinha, A., Cruz, F. W., Wang, X., Edwards, R. L., d'Horta, F. M., et al. (2013). Climate change patterns in Amazonia and biodiversity. *Nat. Commun.* 4, 1411. doi: 10.1038/ncomms2415

Clark, J. S., Lynch, J., Stocks, B. J., and Goldammer, J. G. (1998). Relationships between charcoal particles in air and sediments in west-central Siberia. *Sage J.* 1, 19–29. doi: 10.1191/095968398672501165

Clement, C. R., de Cristo-Araújo, M., Coppens D'Eeckenbrugge, G., Alves Pereira, A., and Picanço-Rodrigues, D. (2010). Origin and domestication of native Amazonian crops. *Diversity* 2, 72–106. doi: 10.3390/d2010072

Clement, C. R., Denevan, W. M., Heckenberger, M. J., Junqueira, A. B., Neves, E. G., Teixeira, W. G., et al. (2015). The domestication of Amazonia before European conquest. *Proc. R. Soc. Lond. B Biol. Sci.* 282, 20150813. doi: 10.1098/rspb.2015.0813

Cloern, J. E., Canuel, E. A., and Harris, D. (2002). Stable carbon and nitrogen isotope composition of aquatic and terrestrial plants of the San Francisco Bay estuarine system. *Limnol. Oceanogr.* 47, 713–729. doi: 10.4319/lo.2002.47.3.0713

Cochrane, M. A. (ed.). (2009). "Fire in the tropics," in *Tropical Fire Ecology* (Berlin: Springer), 1–23. doi: 10.1007/978-3-540-77381-8_1

Cochrane, M. A., and Ryan, K. C. (2009). "Fire and fire ecology: concepts and principles," in *Tropical Fire Ecology*, ed. M. A. Cochrane (Berlin: Springer), 25–62. doi: 10.1007/978-3-540-77381-8

Codron, J., Codron, D., Lee-Thorp, J. A., Sponheimer, M., Bond, W. J., de Ruiter, D., et al. (2005). Taxonomic, anatomical, and spatio-temporal variations in the stable carbon and nitrogen isotopic compositions of plants from an African savanna. *J. Archaeol. Sci.* 32, 1757–1772. doi: 10.1016/j.jas.2005.06.006

Crema, E. (2022). Statistical inference of prehistoric demography from frequency distributions of radiocarbon dates: a review and a guide for the perplexed. *J. Archaeol. Method Theory* 29, 1387–1418. doi: 10.1007/s10816-022-09559-5

Crema, E. R., and Bevan, A. (2021). Inference from large sets of radiocarbon dates: software and methods. *Radiocarbon* 63, 23–39. doi: 10.1017/RDC.2020.95

Croudace, I. W., Rindby, A., and Rothwell, R. G. (2006). ITRAX: description and evaluation of a new multi-function X-ray core scanner. *Spec. Publ.-Geol. Soc. London* 267, 51. doi: 10.1144/GSL.SP.2006.267.01.04

Cruz, F. W., Burns, S. J., and Karmann, I. (2005). Insolation-driven changes in atmospheric circulation over the past 116,000 years in subtropical Brazil. *Nature* 434, 63–66. doi: 10.1038/nature03365

Cruz, F. W., Vuille, M., Burns, S. J., Wang, X., Cheng, H., Werner, M., et al. (2009). Orbitally driven east–west antiphasing of South American precipitation. *Nat. Geosci.* 2, 210–214. doi: 10.1038/ngeo444

de Cristo-Araújo, M., Maciel dos Reis, V., Picanço Rodrigues, D., and Clement, C. R. (2013). Domestication of Peach Palm in Southwestern Amazonia. *Tipití* 11, 74–80. Available online at: https://digitalcommons.trinity.edu/tipiti/vol11/iss2/9

de Souza, J. G., Robinson, M., Maezumi, S. Y., Capriles, J., Hoggarth, J. A., Lombardo, U., et al. (2019). Climate change and cultural resilience in late pre-Columbian Amazonia. *Nat. Ecol. Evol.* 3, 1007–1017. doi: 10.1038/s41559-019-0924-0

Dean Jr, W. E. (1974). Determination of carbonate and organic matter in calcareous sediments and sedimentary rocks by loss on ignition: comparison with other methods. *J. Sediment. Res.* 44, 242–248. doi: 10.1306/74D729D2-2B21-11D7-8648000102C1865D

Denevan, W. (2005). Charles mann and humanized landscapes. *Geogr. Rev.* 96, 483–487. doi: 10.1111/j.1931-0846.2006.tb00267.x

Denevan, W. M. (1996). A bluff model of riverine settlement in prehistoric Amazonia. *Ann. Am. Assoc. Geogr.* 86, 654–681. doi: 10.1111/j.1467-8306.1996.tb01771.x

Denevan, W. M. (2006). "Time and complexity in historical ecology," in *Studies in the Neotropical Lowlands*, eds W. Balée and C. L. Erickson (Columbia University Press), 153–164. doi: 10.7312/bale13562-008

Doughty, C. E., Metcalfe, D. B., Girardin, C. A. J., Amézquita, F. F., Cabrera, D. G., Huasco, W. H., et al. (2015). Drought impact on forest carbon dynamics and fluxes in Amazonia. *Nature* 519, 78. doi: 10.1038/nature14213

Downey, S. S., Haas, W. R., and Shennan, S. J. (2016). European Neolithic societies showed early warning signals of population collapse. *Proc. Nat. Acad. Sci.* 113, 9751–9756. doi: 10.1073/pnas.1602504113

Duffin, K. I., Gillson, L., and Willis, K. J. (2008). Testing the sensitivity of charcoal as an indicator of fire events in savanna environments: quantitative predictions of fire proximity, area and intensity. *Holocene* 2, 279–291. doi: 10.1177/0959683607086766

Edwards, E. J., Osborne, C. P., Strömberg, C. A. E., Smith, S. A., null, null, Bond, W. J., et al. (2010). The origins of C4 grasslands: integrating evolutionary and ecosystem science. *Science* 328, 587–591. doi: 10.1126/science.1177216

Ehleringer, J., and Björkman, O. (1977). Quantum yields for CO(2) uptake in C(3) and C(4) plants: dependence on temperature, CO(2), and O(2) concentration. *Plant Physiol.* 59, 86–90. doi: 10.1104/pp.59.1.86

Ehleringer, J. R., Buchmann, N., and Flanagan, L. B. (2000). Carbon isotope ratios in belowground carbon cycle processes. *Ecol. Appl.* 10, 412–422. doi: 10.1890/1051-0761(2000)010[0412:CIRIBC]2.0.CO;2

Ehleringer, J. R., and Cerling, T. E. (2002). "C3 and C4 photosynthesis," in *Encyclopedia of Global Environmental Change. 2. The Earth System: Biological and Ecological Dimensions of Global Environmental Change*, eds H. A. Mooney, and T. Munn (Hoboken, NJ: Wiley), 186–190.

Ehleringer, J. R., Sage, R. F., Flanagan, L. B., and Pearcy, R. W. (1991). Climate change and the evolution of C4 photosynthesis. *Trends Ecol. Evol.* 6, 95–99. doi: 10.1016/0169-5347(91)90183-X

Feldpausch, T. R., Phillips, O. L., Brienen, R. J. W., Gloor, E., Lloyd, J., Lopez-Gonzalez, G., et al. (2016). Amazon forest response to repeated droughts. *Global Biogeochem. Cycles* 30, 964–982. doi: 10.1002/2015GB005133

Furquim, L. P., Neves, E. G., Shock, M. P., and Watling, J. (2023). "The constructed biodiversity, forest management and use of fire in ancient Amazon: an archaeological testimony on the last 14,000 years of indigenous history," in *Global Ecology in Historical Perspective: Monsoon Asia and Beyond*, eds K. Ikeya, and W. Balée (Singapore: Springer Nature Singapore), 259–281. doi: 10.1007/978-981-19-6557-9_15

Furquim, L. P., Watling, J., Hilbert, L. M., Shock, M. P., Prestes-Carneiro, G., Calo, C. M., et al. (2021). Facing change through diversity: resilience and diversification of plant management strategies during the mid to late Holocene transition at the Monte Castelo Shellmound, SW Amazonia. *Quaternary* 4, 1–29. doi: 10.3390/quat4010008

Gedye, S. J., Jones, R. T., Tinner, W., Ammann, B., and Oldfield, F. (2000). The use of mineral magnetism in the reconstruction of fire history: a case study from Lago di Origlio, Swiss Alps. *Palaeogeogr. Palaeoclimatol. Palaeoecol.* 164, 101–110. doi: 10.1016/S0031-0182(00)00178-4

Glaser, B., and Woods, W. I. (2004). *Amazonian Dark Earths: Explorations in Space and Time*. Berlin: Springer. doi: 10.1007/978-3-662-05683-7

Goldberg, A., Mychajliw, A. M., and Hadly, E. A. (2016). Post-invasion demography of prehistoric humans in South America. *Nature* 532, 232–235. doi: 10.1038/nature17176

Haug, G. H., Hughen, K. A., Sigman, D. M., Peterson, L. C., and Röhl, U. (2001). Southward migration of the intertropical convergence zone through the Holocene. *Science* 293, 1304–1308. doi: 10.1126/science.1059725

Heck, K. L., van Belle, G., and Simberloff, D. (1975). Explicit calculation of the rarefaction diversity measurement and the determination of sufficient sample size. *Ecology* 56, 1459–1461. doi: 10.2307/1934716

Heckenberger, M., and Neves, E. G. (2009). Amazonian archaeology. *Annu. Rev. Anthropol.* 38, 251–266. doi: 10.1146/annurev-anthro-091908-164310

Heckenberger, M. J., Russell, J. C., Fausto, C., Toney, J. R., Schmidt, M. J., Pereira, E., et al. (2008). Pre-Columbian urbanism, anthropogenic landscapes, and the future of the Amazon. *Science* 321, 1214–1217. doi: 10.1126/science.1159769

Heiri, O., Lotter, A. F., and Lemcke, G. (2001). Loss on ignition as a method for estimating organic and carbonate content in sediments: reproducibility and comparability of results. *J. Paleolimnol.* 25, 101–110. doi: 10.1023/A:1008119611481

Heyer, J. P., Power, M. J., Field, R. D., and Van Marle, M. J. E. (2018). The impacts of recent drought on fire, forest loss, and regional smoke emissions in lowland Bolivia. *Biogeosciences* 15, 4317–4331. doi: 10.5194/bg-15-4317-2018

Higuera, P., Peters, M., Brubaker, L., and Gavin, D. (2007). Understanding the origin and analysis of sediment-charcoal records with a simulation model. *Quat. Sci. Rev.* 26, 1790–1809. doi: 10.1016/j.quascirev.2007.03.010

Higuera, P. E., Brubaker, L. B., Anderson, P. M., Feng, S. H., and Brown, T. A. (2009). Vegetation mediated the impacts of postglacial climate change on fire regimes in the south-central Brooks Range, Alaska. *Ecol. Monogr.* 79, 201–219. doi: 10.1890/07-2019.1

Higuera, P. E., Whitlock, C., and Gage, J., a. (2010). Linking tree-ring and sediment-charcoal records to reconstruct fire occurrence and area burned in subalpine forests of Yellowstone National Park, USA. *Holocene* 21, 327–341. doi: 10.1177/0959683610374882

Hilbert, L., Neves, E. G., Pugliese, F., Whitney, B. S., Shock, M., Veasey, E., et al. (2017). Evidence for mid-Holocene rice domestication in the Americas. *Nat. Ecol. Evol.* 1, 1693–1698. doi: 10.1038/s41559-017-0322-4

Hoetzel, S., Dupont, L., Schefu,ß, E., Rommerskirchen, F., and Wefer, G. (2013). The role of fire in Miocene to Pliocene C4 grassland and ecosystem evolution. *Nat. Geosci.* 6, 1027. doi: 10.1038/ngeo1984

Hoffman, K. M., Davis, E. L., Wickham, S. B., Schang, K., Johnson, A., Larking, T., et al. (2021). Conservation of Earth's biodiversity is embedded in Indigenous fire stewardship. *Proc. Nat. Acad. Sci.* 118, e2105073118. doi: 10.1073/pnas.2105073118

Hogg, A. G., Hua, Q., Blackwell, P. G., Niu, M., Buck, C. E., Guilderson, T. P., et al. (2013). SHCal13 Southern Hemisphere calibration, 0–50,000 years cal BP. *Radiocarbon* 55, 1889–1903. doi: 10.2458/azu_js_rc.55.16783

Hurlbert, S. H. (1971). The nonconcept of species diversity: a critique and alternative parameters. *Ecology* 52, 577–586. doi: 10.2307/1934145

Iriarte, J., Elliott, S., Maezumi, S. Y., Alves, D., Gonda, R., Robinson, M., et al. (2020). The origins of Amazonian landscapes: Plant cultivation, domestication and the spread of food production in tropical South America. *Quat. Sci. Rev.* 248, 106582. doi: 10.1016/j.quascirev.2020.106582

Jepson, W. L. (1993). The Jepson *Manual: Higher Plants of California*. Berkeley, CA: University of California Press.

Jordan, C., Caskey, W., Escalante, G., Herrera, R., Montagnini, F., Todd, R., et al. (1982). "The nitrogen cycle in a 'Terra Firme' rainforest on oxisol in the Amazon territory of Venezuela," in *Nitrogen Cycling in Ecosystems of Latin America and the Caribbean*, eds G. P. Robertson, R. Herrera, and T. Rosswall (Dordrecht: Springer Netherlands), 325–332. doi: 10.1007/978-94-009-7639-9_29

Junqueira, A. B., Shepard, G. H., and Clement, C. R. (2010). Secondary forests on anthropogenic soils in Brazilian Amazonia conserve agrobiodiversity. *Biodivers. Conserv.* 19, 1933–1961. doi: 10.1007/s10531-010-9813-1

Kanner, L. C., Burns, S. J., Cheng, H., Edwards, R. L., and Vuille, M. (2013). High-resolution variability of the South American summer monsoon over the last seven millennia: insights from a speleothem record from the central Peruvian Andes. *Quat. Sci. Rev.* 75, 1–10. doi: 10.1016/j.quascirev.2013.05.008

Keeley, J. E., and Rundel, P. W. (2005). Fire and the Miocene expansion of C4 grasslands. *Ecol. Lett.* 8, 683–690. doi: 10.1111/j.1461-0248.2005.00767.x

Keeley, J. E., and Sandquist, D. (1992). Carbon: freshwater plants. *Plant Cell Environ.* 15, 1021–1035. doi: 10.1111/j.1365-3040.1992.tb01653.x

Killeen, T. J. (1998). "Geomorphology of the Huanchaca Plateau and surrounding areas," in *A Biological Assessment of Parque Nacional Noel Kempff Mercado, Bolivia*, eds T. J. Killeen, and T. S. Schulenberg (Washington, DC: Conservation International), 43–46.

Killeen, T. J., and Schulenberg, T. S. (1998). *Vegetation and flora of Noel Kempff Mercado National Park. A biological assessment of Parque Nacional Noel Kempff Mercado, Bolivia*. RAP working papers 10. Washington, DC: Conservation International.

Killeen, T. J., Siles, T. M., Grimwood, T., Tieszen, L. L., Steininger, M. K., Tucker, C. J., et al. (2003). "Habitat heterogeneity on a forest-savanna ecotone in Noel Kempff Mercado National Park (Santa Cruz, Bolivia): Implications for the long-term conservation of biodiversity in a changing climate," in *How Landscapes Change Ecological Studies*, eds G. A. Bradshaw, and P. A. Marquet (Berlin: Springer Verlag), 285–312. doi: 10.1007/978-3-662-05238-9_17

Kirschner, J., and Hoorn, C. (2019). The onset of grasses in the Amazon drainage basin, evidence from the fossil record. *Front. Biogeogr.* 12, 44827. doi: 10.21425/F5FBG44827

Kistler, L., Maezumi, S. Y., Gregorio de Souza, J., Przelomska, N. A. S., Malaquias Costa, F., Smith, O., et al. (2018). Multiproxy evidence highlights a complex evolutionary legacy of maize in South America. *Science* 362, 1309–1313. doi: 10.1126/science.aav0207

Kohn, M. J. (2010). Carbon isotope compositions of terrestrial C3 plants as indicators of (paleo)ecology and (paleo)climate. *Proc. Nat. Acad. Sci.* 107, 19691–19695. doi: 10.1073/pnas.1004933107

Latrubesse, E. M., Stevaux, J. C., Cremon, E. H., May, J.-H., Tatumi, S. H., Hurtado, M. A., et al. (2012). Late quaternary megafans, fans and fluvio-aeolian interactions in the Bolivian Chaco, tropical South America. *Palaeogeogr. Palaeoclimatol. Palaeoecol.* 356, 75–88. doi: 10.1016/j.palaeo.2012.04.003

Le Page, Y., Morton, D., Corinne, H., Ben, B.-L., Cardoso Pereira, J. M., Hurtt, G., et al. (2017). Synergy between land use and climate change increases future fire risk in Amazon forests. *Earth Syst. Dyn. Discuss.* 8, 1–19. doi: 10.5194/esd-2017-55

Lehmann, J., Kern, D. C., Glaser, B., and Woods, W. I. (2003). *Amazonian Dark Earths: Origin Properties Management*. Amsterdam: Springer Netherlands. doi: 10.1007/1-4020-2597-1

Lenton, T. M., Rockström, J., Gaffney, O., Rahmstorf, S., Richardson, K., Steffen, W., et al. (2019). Climate tipping points - too risky to bet against. *Nature* 575, 592–595. doi: 10.1038/d41586-019-03595-0

Levis, C., Flores, B. M., Moreira, P. A., Luize, B. G., Alves, R. P., Franco-Moraes, J., et al. (2018). How people domesticated Amazonian forests. *Front. Ecol. Evol.* 5, 171. doi: 10.3389/fevo.2017.00171

Leys, B., Brewer, S. C., McConaghy, S., Mueller, J., and McLauchlan, K. K. (2015). Fire history reconstruction in grassland ecosystems: amount of charcoal reflects local area burned. *Environ. Res. Lett.* 10, 114009. doi: 10.1088/1748-9326/10/11/114009

Lins, J., Lima, H. P., Baccaro, F. B., Kinupp, V. F., Shepard, G. H. Jr, Clement, C. R. (2015). Pre-Columbian floristic legacies in modern homegardens of Central Amazonia. *PLoS ONE* 10, e0127067. doi: 10.1371/journal.pone.0127067

Lombardo, U., Iriarte, J., Hilbert, L., Ruiz-Pérez, J., Capriles, J. M., and Veit, H. (2020). Early Holocene crop cultivation and landscape modification in Amazonia. *Nature* 581, 190–193. doi: 10.1038/s41586-020-2162-7

Lombardo, U., Rodrigues, L., and Veit, H. (2018). Alluvial plain dynamics and human occupation in SW Amazonia during the Holocene: a paleosol-based reconstruction. *Quat. Sci. Rev.* 180, 30–41. doi: 10.1016/j.quascirev.2017.11.026

Lombardo, U., Ruiz-Pérez, J., Rodrigues, L., Mestrot, A., Mayle, F., Madella, M., et al. (2019). Holocene land cover change in south-western Amazonia inferred from paleoflood archives. *Glob. Planet. Change* 174, 105–114. doi: 10.1016/j.gloplacha.2019.01.008

Lombardo, U., Szabo, K., Capriles, J. M., May, J.-H., Amelung, W., Hutterer, R., et al. (2013). Early and middle holocene hunter-gatherer occupations in Western Amazonia: the Hidden Shell Middens. *PLoS ONE* 8, e72746. doi: 10.1371/journal.pone.0072746

Loughlin, N. J. D., Gosling, W. D., Mothes, P., and Montoya, E. (2018). Ecological consequences of post-Columbian indigenous depopulation in the Andean–Amazonian corridor. *Nat. Ecol. Evol.* 2, 1233–1236. doi: 10.1038/s41559-018-0602-7

Lynch, J. A., Clark, J. S., and Stocks, B. J. (2004). Charcoal production, dispersal, and deposition from the Fort Providence experimental fire: interpreting fire regimes from charcoal records in boreal forests. *Can. J. For. Res.* 1656, 1642–1656. doi: 10.1139/x04-071

Maezumi, S. Y., Elliott, S., Robinson, M., Jaimes Betancourt, C., Gregorio de Souza, J., Alves, D., et al. (2022). Legacies of Indigenous land use and cultural burning in the Bolivian Amazon rainforest ecotone. *Phil. Trans. R. Soc. B.* 377, 20200499. doi: 10.1098/rstb.2020.0499

Maezumi, S. Y., Power, M. J., Mayle, F. E., McLauchlan, K. K., and Iriarte, J. (2015). Effects of past climate variability on fire and vegetation in the cerrādo savanna of the Huanchaca Mesetta, NE Bolivia. *Clim. Past* 11, 835–853. doi: 10.5194/cp-11-835-2015

Maezumi, S. Y., Robinson, M., Gregorio de Souza, J., Urrego, D., Schaan, D., Alves, D., et al. (2018a). New insights from pre-Columbian land use and fire management in Amazonian Dark Earth forests. *Front. Ecol. Evol.* 6, 1–23. doi: 10.3389/fevo.2018.00111

Maezumi, S. Y., Whitney, B. S., Mayle, F. E., Gregorio de Souza, J., and Iriarte, J. (2018b). Reassessing climate and pre-Columbian drivers of paleofire activity in the Bolivian Amazon. *Quat. Int.* 488, 81–94. doi: 10.1016/j.quaint.2017.11.053

Marlon, J. R., Bartlein, P. J., Daniau, A., Harrison, S. P., Maezumi, S. Y., Power, M. J., et al. (2013). Global biomass burning: a synthesis and review of Holocene paleofire records and their controls. *Quat. Sci. Rev.* 65, 5–25. doi: 10.1016/j.quascirev.2012.11.029

Mayle, F. E., Beerling, D. J., Gosling, W. D., and Bush, M. B. (2004). Responses of Amazonian ecosystems to climatic and atmospheric carbon dioxide changes since the last glacial maximum. *Philos. Trans. R. Soc. Lond. B Biol. Sci.* 359, 499–514. doi: 10.1098/rstb.2003.1434

Mayle, F. E., Burbridge, R. E., and Killeen, T. J. (2000). Millennial-scale dynamics of southern Amazonian rain forests. *Science* 290, 2291–2294. doi: 10.1126/science.290.5500.2291

Mayle, F. E., Langstroth, R. P., Fisher, R., a, and Meir, P. (2007). Long-term forest-savannah dynamics in the Bolivian Amazon: implications for conservation. *Philos. Trans. R. Soc. Lond. B Biol. Sci.* 362, 291–307. doi: 10.1098/rstb.2006.1987

Mayle, F. E., and Power, M. J. (2008). Impact of a drier Early-Mid-Holocene climate upon Amazonian forests. *Philos. Trans. R. Soc. Lond. B Biol. Sci.* 363, 1829–1838. doi: 10.1098/rstb.2007.0019

Mayle, F. E., and Whitney, B. S. (2012). "Long-term perspectives on tropical forest-savanna dynamics in lowland Bolivia from the last ice age until present," in *Ecotones Between Forest and Grassland*, ed. R. W. Myster (London: Springer), 189–207. doi: 10.1007/978-1-4614-3797-0_8

McCormac, F. G., Hogg, A. G., Blackwell, P. G., Buck, C. E., Higham, T. F. G., and Reimer, P. J. (2004). SHCAL04 southern hemisphere calibration, 0-11.0 cal KYR BP. *Radiocarbon* 46, 1087–1092. doi: 10.1017/S0033822200033014

McLauchlan, K. K., Lascu, I., Myrbo, A., and Leavitt, P. R. (2013). Variable ecosystem response to climate change during the Holocene in northern Minnesota, USA. *Geol. Soc. Am. Bull.* 23, 1635–1643. doi: 10.1130/B30737.1

McMichael, C. H., Palace, M. W., Bush, M. B., Braswell, B., Hagen, S., Neves, E. G., et al. (2014). Predicting pre-Columbian anthropogenic soils in Amazonia. *Proc. R. Soc. B Biol. Sci.* 281, 20132475. doi: 10.1098/rspb.2013.2475

McMichael, C. N. H., and Bush, M. B. (2019). Spatiotemporal patterns of pre-Columbian people in Amazonia. *Quat. Res.* 92, 53–69. doi: 10.1017/qua.2018.152

Metcalfe, S. E., Whitney, B. S., Fitzpatrick, K. A., Mayle, F. E., Loader, N. J., Street-Perrott, F. A., et al. (2014). Hydrology and climatology at Laguna La Gaiba, lowland Bolivia: Complex responses to climatic forcings over the last 25 000 years. *J. Quat. Sci.* 29, 289–300. doi: 10.1002/jqs.2702

Monnin, E., Indermühle, A., Dällenbach, A., Flückiger, J., Stauffer, B., Stocker, T. F., et al. (2001). Atmospheric CO_2 concentrations over the last glacial termination. *Science* 291, 112–114. doi: 10.1126/science.291.5501.112

Mora, S., Herrera, L. F., Cavalier, I., and Rodríguez, C. (1991). *Cultivars, Anthropic Soils, and Stability: A Preliminary Report of Archaeological Research in Araracuara, Colombian Amazonia*. Pittsburgh, PA: Center for Comparative Archaeology.

Neves, E. G. (2012). *Sob os Tempos do Equinócio: Oito mil Anos de história na Amazônia Central (6.500 AC-1.500 DC)*. São Paulo: Universidade de São Paulo.

Novello, V. F., Cruz, F. W., McGlue, M. M., Wong, C. I., Ward, B. M., Vuille, M., et al. (2019). Vegetation and environmental changes in tropical South America from the last glacial to the Holocene documented by multiple cave sediment proxies. *Earth Planet. Sci. Lett.* 524, 115717. doi: 10.1016/j.epsl.2019.115717

Novello, V. F., Cruz, F. W., Vuille, M., Stríkis, N. M., Edwards, R. L., Cheng, H., et al. (2017). A high-resolution history of the South American monsoon from Last Glacial Maximum to the Holocene. *Sci. Rep.* 7, 44267. doi: 10.1038/srep44267

Nowaczyk, N. R. (2001). "Logging of magnetic susceptibility," in *Tracking Environmental Change using Lake Sediments*, eds. J. P. Smol, H. J. B. Birks, and W. M. Last (Potsdam: Springer Netherlands), 155–170. doi: 10.1007/0-306-47669-X_8

O'Connor, C., Garfin, G., Falk, D., and Swetnam, T. (2011). Human pyrogeography: a new synergy of fire, climate and people is reshaping ecosystems across the globe. *Geogr. Compass* 5/6, 329–350. doi: 10.1111/j.1749-8198.2011.00428.x

Oksanen, J., Blanchet, F. G., Friendly, M., Kindt, R., Legendre, P., McGlinn, D., et al. (2017). *Package "Vegan" Community Ecology. Package Version* 2–5.

O'Leary, M. H. (1981). Carbon isotope fractionation in plants. *Phytochemistry* 20, 553–567. doi: 10.1016/0031-9422(81)85134-5

O'Leary, M. H. (1988). Carbon isotopes in photosynthesis. *Bioscience* 38, 328–336. doi: 10.2307/1310735

Oliver, J. R. (2008). "The archaeology of agriculture in ancient Amazonia," in *The Handbook of South American Archaeology*, eds H. Silverman, and W. H. Isbell (New York, NY: Springer), 185–216. doi: 10.1007/978-0-387-74907-5_12

Olson, D. M., and Dinerstein, E. (2002). The Global 200: priority ecoregions for global conservation. *Ann. Missouri Bot. Gard.* 89, 199–224. doi: 10.2307/3298564

Ometto, J. P. H. B., Ehleringer, J. R., Domingues, T. F., Berry, J. A., Ishida, F. Y., Mazzi, E., et al. (2006). "The stable carbon and nitrogen isotopic composition of vegetation in tropical forests of the Amazon Basin, Brazil," in *Nitrogen Cycling in the Americas: Natural and Anthropogenic Influences and Controls*, eds L. A. Martinelli, and R. W. Howarth (Dordrecht: Springer), 251–274. doi: 10.1007/978-1-4020-5517-1_12

Oris, F., Ali, A. A., Asselin, H., Paradis, L., Bergeron, Y., and Finsinger, W. (2014). Charcoal dispersion and deposition in boreal lakes from 3 years of monitoring: differences between local and regional fires. *Geophys. Res. Lett.* 41, 6743–6752. doi: 10.1002/2014GL060984

Orrison, R., Vuille, M., Smerdon, J. E., Apaéstegui, J., Azevedo, V., Campos, J. L. P., et al. (2022). South American Summer Monsoon variability over the last millennium in paleoclimate records and isotope-enabled climate models. *Clim. Past* 18, 2045–2062. doi: 10.5194/cp-18-2045-2022

Pereira, J. M. C., Oom, D., Silva, P. C., and Benali, A. (2022). Wild, tamed, and domesticated: three fire macroregimes for global pyrogeography in the Anthropocene. *Ecol. Appl.* 32, e2588. doi: 10.1002/eap.2588

Peripato, V., Levis, C., Moreira, G. A., Gamerman, D., ter Steege, H., Pitman, N. C. A., et al. (2023). More than 10,000 pre-Columbian earthworks are still hidden throughout Amazonia. *Science* 382, 103–109. doi: 10.1126/science.ade2541

Pessenda, L. C. R., Gouveia, S. E. M., Gomes, B. M., Aravena, R., Ribeiro, A. S., and Boulet, R. (1998). The carbon isotope record in soils along a forest-cerrado ecosystem transect: implications for vegetation changes in the Rondonia state, southwestern Brazilian Amazon region. *Holocene* 8, 599–603. doi: 10.1191/095968398673187182

Politis, G. G. (1996). Moving to produce: Nukak mobility and settlement patterns in Amazonia. *World Archaeol.* 27, 492–511. doi: 10.1080/00438243.1996.9980322

Posey, D. A., and Balée, W. L. (1989). Resource *Management* in *Amazonia: Indigenous and Folk Strategies*. New York, NY: New York Botanical Garden.

Power, M. J., Marlon, J. R., Bartlein, P. J., and Harrison, S. P. (2010). Fire history and the Global Charcoal Database: a new tool for hypothesis testing and data exploration. *Palaeogeogr. Palaeoclimatol. Palaeoecol.* 291, 52–59. doi: 10.1016/j.palaeo.2009.09.014

Power, M. J., Whitney, B. S., Mayle, F. E., Neves, D. M., de Boer, E. J., and Maclean, K. S. (2016). Fire, climate and vegetation linkages in the Bolivian Chiquitano seasonally dry tropical forest. *Phil. Trans. R. Soc. B* 371, 20150165. doi: 10.1098/rstb.2015.0165

Price, M. H., Capriles, J. M., Hoggarth, J. A., Bocinsky, R. K., Ebert, C. E., and Jones, J. H. (2021). End-to-end Bayesian analysis for summarizing sets of radiocarbon dates. *J. Archaeol. Sci.* 135, 105473. doi: 10.1016/j.jas.2021.105473

Pyne, S. J. (2021). *The Pyrocene*. Berkeley, CA: University of California Press. doi: 10.1525/9780520383593

R Core Development Team (2020). R: A *Language* and *Environment* for *Statistical Computing*. Vienna: R Foundation for Statistical Computing R Foundation for Statistical Computing

Ramos-Neto, M. B., and Pivello, V. R. (2000). Lightning fires in a Brazilian savanna National Park: Rethinking management strategies. *Environ. Manage.* 26, 675–684. doi: 10.1007/s002670010124

Ramsey, C. B. (2017). Methods for summarizing radiocarbon datasets. *Radiocarbon* 59, 1809–1833. doi: 10.1017/RDC.2017.108

Reimer, P. J. (2020). Composition and consequences of the IntCal20 radiocarbon calibration curve. *Quat. Res.* 96, 22–27. doi: 10.1017/qua.2020.42

Reimer, P. J., Austin, W. E. N., Bard, E., Bayliss, A., Blackwell, P. G., Bronk Ramsey, C., et al. (2020). The IntCal20 Northern hemisphere radiocarbon age calibration curve (0–55 cal kBP). *Radiocarbon* 62, 725–757. doi: 10.1017/RDC.2020.41

Rick, J. W. (1987). Dates as data: an examination of the Peruvian preceramic radiocarbon record. *Am. Antiq.* 52, 55–73. doi: 10.2307/281060

Riester, J. G. (1981). *Arqueología y Arte Rupestre en el Oriente Boliviano*. Cochabamba La Paz: Editorial Los Amigos del Libro.

Roberts, P., Hunt, C., Arroyo-Kalin, M., Evans, D., and Boivin, N. L. (2017). The deep human prehistory of global tropical forests and its relevance for modern conservation. *Nat. Plants* 3, 17093. doi: 10.1038/nplants.2017.93

Roberts, P., Lee-Thorp, J. A., Mitchell, P. J., and Arthur, C. (2013). Stable carbon isotopic evidence for climate change across the late Pleistocene to early Holocene from Lesotho, southern Africa. *J. Quat. Sci.* 28, 360–369. doi: 10.1002/jqs.2624

Robinson, D. (1991). *Roots and Resources Fluxes in Plant and Communities*. Oxford: Blackwell Scientific Publications.

Sage, R. F. (2004). The evolution of C4 photosynthesis. *New Phytol.* 161, 341–370. doi: 10.1111/j.1469-8137.2004.00974.x

Sage, R. F., and Kubien, D. S. (2007). The temperature response of C3 and C4 photosynthesis. *Plant Cell Environ.* 30, 1086–1106. doi: 10.1111/j.1365-3040.2007.01682.x

Sato, H., Kelley, D. I., Mayor, S. J., Martin Calvo, M., Cowling, S. A., and Prentice, I. C. (2021). Dry corridors opened by fire and low CO_2 in Amazonian rainforest during the Last Glacial Maximum. *Nat. Geosci.* 14, 578–585. doi: 10.1038/s41561-021-00777-2

Seitzinger, S., Harrison, J. A., Böhlke, J. K., Bouwman, A. F., Lowrance, R., Peterson, B., et al. (2006). Denitrification across landscapes and waterscapes: a synthesis. *Ecol. Appl.* 16, 2064–2090. doi: 10.1890/1051-0761(2006)016[2064:DALAWA]2.0.CO;2

Seltzer, G. O., Rodbell, D. T., Baker, P. A., Fritz, S. C., Tapia, P. M., Rowe, H. D., et al. (2002). Early warming of tropical South America at the last glacial-interglacial transition. *Science* 296, 1685–1686. doi: 10.1126/science.1070136

Servant-Vildary, S., Servant, M., and Jimenez, O. (2001). Holocene hydrological and climatic changes in the southern Bolivian Altiplano according to diatom assemblages in paleowetlands. *Hydrobiologia* 466, 267–277. doi: 10.1023/A:1014557417689

Sharkey, T. D., Berry, J. A., and Raschke, K. (1985). Starch and sucrose synthesis in Phaseolus vulgaris as affected by light, CO_2, and abscisic acid. *Plant Physiol.* 77, 617–620. doi: 10.1104/pp.77.3.617

Shennan, S., Downey, S. S., Timpson, A., Edinborough, K., Colledge, S., Kerig, T., et al. (2013). Regional population collapse followed initial agriculture booms in mid-Holocene Europe. *Nat. Commun.* 4, 1–8. doi: 10.1038/ncomms3486

Sifeddine, A., Martin, L., Turcq, B., Volkmer-Ribeiro, C., Soubiès, F., Cordeiro, R. C., et al. (2001). Variations of the Amazonian rainforest environment: a sedimentological record covering 30,000 years. *Palaeogeogr. Palaeoclimatol. Palaeoecol.* 168, 221–235. doi: 10.1016/S0031-0182(00)00256-X

Smith, B. N., and Epstein, S. (1971). Two categories of c/c ratios for higher plants. *Plant Physiol.* 47, 380–384. doi: 10.1104/pp.47.3.380

Smith, R. J., Mayle, F. E., Maezumi, S. Y., and Power, M. J. (2021). Relating pollen representation to an evolving Amazonian landscape between the Last Glacial Maximum and Late Holocene. *Quat. Res.* 99, 63–79. doi: 10.1017/qua.2020.64

Street-Perrott, F. A., Ficken, K. J., Huang, Y., and Eglinton, G. (2004). Late Quaternary changes in carbon cycling on Mt. Kenya, East Africa: an overview of the δ13C record in lacustrine organic matter. *Quat. Sci. Rev.* 23, 861–879. doi: 10.1016/j.quascirev.2003.06.007

Strömberg, C. E. (2011). Evolution of grasses and grassland ecosystems. *Annu. Rev. Earth Planet. Sci.* 39, 517–544. doi: 10.1146/annurev-earth-040809-152402

Tejada, J. V., Flynn, J. J., Antoine, P.-O., Pacheco, V., Salas-Gismondi, R., and Cerling, T. E. (2020). Comparative isotope ecology of western Amazonian rainforest mammals. *Proc. Nat. Acad. Sci.* 117, 26263–26272. doi: 10.1073/pnas.2007440117

ter Steege, H., Pitman, N. C., a, Sabatier, D., Baraloto, C., Salomão, R. P., Guevara, J. E., et al. (2013). Hyperdominance in the Amazonian tree flora. *Science* 342, 1243092. doi: 10.1126/science.1243092

Timpson, A., Colledge, S., Crema, E., Edinborough, K., Kerig, T., Manning, K., et al. (2014). Reconstructing regional population fluctuations in the European Neolithic using radiocarbon dates: a new case-study using an improved method. *J. Archaeol. Sci.* 52, 549–557. doi: 10.1016/j.jas.2014.08.011

Urrego, D. H., Bush, M. B., Silman, M. R., Niccum, B. A., De La Rosa, P., McMichael, C. H., et al. (2013). Holocene fires, forest stability and human occupation in south-western Amazonia. *J. Biogeogr.* 40, 521–533. doi: 10.1111/jbi.12016

Vachula, R. S., and Rehn, E. (2023). Modeled dispersal patterns for wood and grass charcoal are different: Implications for paleofire reconstruction. *Holocene* 33, 159–166. doi: 10.1177/09596836221131708

Vachula, R. S., Sae-Lim, J., and Li, R. (2021). A critical appraisal of charcoal morphometry as a paleofire fuel type proxy. *Quat. Sci. Rev.* 262, 106979. doi: 10.1016/j.quascirev.2021.106979

Vuille, M., Burns, S. J., Taylor, B. L., Cruz, F. W., Bird, B. W., Abbott, M. B., et al. (2012). A review of the South American monsoon history as recorded in stable isotopic proxies over the past two millennia. *Clim. Past* 8, 1309–1321. doi: 10.5194/cp-8-1309-2012

Wang, X., Auler, A. S., Edwards, R. L., Cheng, H., Ito, E., Wang, Y., et al. (2007). Millennial-scale precipitation changes in southern Brazil over the past 90,000 years. *Geophys. Res. Lett.* 34, 237–201. doi: 10.1029/2007GL031149

Watling, J., Shock, M. P., Mongel,ó, G. Z., Almeida, F. O., Kater, T., De Oliveira, P. E., et al. (2018). Direct archaeological evidence for Southwestern Amazonia as an early plant domestication and food production centre. *PLoS ONE* 13, e0199868. doi: 10.1371/journal.pone.0199868

Whitlock, C., and Larsen, C. (2001). "Charcoal as a fire proxy," in *Tracking environmental change using Lake Sediments*, eds J. P. Smol, H. J. B. Birks, W. M. Last, R. S. Bradley, and K. Alverson (Dordrecht: Kluwer Academic Publishers), 75–97. doi: 10.1007/0-306-47668-1_5

Whitney, B. S., Mayle, F. E., Punyasena, S. W., Fitzpatrick, K. A., Burn, M. J., Guillen, R., et al. (2011). A 45kyr palaeoclimate record from the lowland interior of tropical South America. *Palaeogeogr. Palaeoclimatol. Palaeoecol.* 307, 177–192. doi: 10.1016/j.palaeo.2011.05.012

Williams, A. (2012). The use of summed radiocarbon probability distributions in archaeology: a review of methods. *J. Archaeol. Sci.* 39, 578–589. doi: 10.1016/j.jas.2011.07.014

Woillez, M.-N., Kageyama, M., Krinner, G., de Noblet-Ducoudré, N., Viovy, N., and Mancip, M. (2011). Impact of CO_2 and climate on the Last Glacial Maximum vegetation: results from the ORCHIDEE/IPSL models. *Clim. Past* 7, 557–577. doi: 10.5194/cp-7-557-2011

Woods, W. I., Teixeira, W. G., Lehmann, J., Steiner, C., WinklerPrins, A., and Rebellato, L. (2009). *Amazonian Dark Earths: Wim Sombroek's Vision*. Berlin: Springer. doi: 10.1007/978-1-4020-9031-8

Wright, H. E. (1967). A square-rod piston sampler for lake sediments. *J. Sediment. Res.* 37, 975–976. doi: 10.1306/74D71807-2B21-11D7-8648000102C1865D

Zahid, H. J., Robinson, E., and Kelly, R. L. (2016). Agriculture, population growth, and statistical analysis of the radiocarbon record. *Proc. Nat. Acad. Sci.* 113, 931–935. doi: 10.1073/pnas.1517650112